A COMPUTATIONAL STUDY ON 18+δ ORGANOMETALLICS

Liwen Yu, B.S.

Thesis Prepared for the Degree of

MASTER OF SCIENCE

UNIVERSITY OF NORTH TEXAS

May 2002

APPROVED:

Martin Schwartz, Major Professor
Paul Marshall, Minor Professor
Ruthanne D. Thomas, Chair of the
Department of Chemistry
C. Neal Tate, Dean of the Robert B. Toulouse
School of Graduate Studies

Yu, Liwen. A Computational Study on 18+δ Organometallics. Master of Science (Chemistry), May 2002, 68 pp., 13 tables, 10 illustrations, bibliography, 70 titles.

The B3LYP density functional has been used to calculate properties of organometallic complexes of $Co(CO)_3$ and $ReBr(CO)_3$, with the chelating ligand 2,3-bisphosphinomaleic anhydride, in 19- and 18-electron forms. The SBKJC-21G effective core potential and associated basis set was used for metals (Co/Re) and the 6-31G* basis set was used for all other elements. The differences of bond angles, bond distances, natural atomic charges and IR vibrational frequencies were compared with the available experimental parameters. The differences between the 19- and 18-electron systems have been analyzed. The results reveal that the 19^{th} electron is mostly distributed over the ligand of 2,3-bisphosphinomaleic anhydride, although partially localized onto the metal fragment in **1** and **2***. Two different methods, IR-frequencies and natural atomic charges, were used to determine the value of δ. Present computed values of δ are compared with available experimental values, and predictions are made for unknown complexes.

TABLE OF CONTENTS

Page

LIST OF TABLES

LIST OF ILLUSTRATIONS

Figure Page

Scheme Page

CHAPTER 1

18+ δ COMPLEXES

A. Introduction

The most fundamental principle of organometallic chemistry is the 18-electron rule [1]. The rule states that a stable organometallic complex contains a total of 18 valence electrons. The reason why this statement can be true is that a transition metal has 9 valence orbitals: five nd orbitals, three (n+1) p orbitals and one (n+1) s orbital. In a complex with n ligands, n of those valence orbitals will be used to form metal-ligand (M-L) σ bonds and the remaining 9-n orbitals will form π bonds or non-bonding molecular orbitals (Fig. 1) [2]. When all σ bonding and π bonding/nonbonding orbitals are filled, one has a total of 18 electrons, which forms a closed-shell around the transition metal. Any additional electrons (greater than 18 valence electrons, e.g., a 19^{th} electron) will have to occupy M-L antibonding orbitals, decreasing the total bond order of the system, which will lead to the instability of the complex. Likewise, any complex with less than 18 valence electrons will also not achieve the maximum bond order, and therefore, is less favorable than complexes obeying the 18-electron rule. Despite the 18-electron rule, there are a number of organometallic complexes known, which have fewer or more than 18 valence electrons. 17-electron complexes, such as $V(CO)_6$, $Mn(CO)_5$ and $Re(CO)_5$, have been generated by photolysis [3]. In addition, the existence of 15-electron and 17-electron intermediates was firmly established

in the late 1970s [4]. 19-electron species were also discovered; for example, cobaltocene, $Co(C_5H_5)_2$, is a well-known 19-electron complex [5].

19-electron complexes are rare because they are high in energy with an electron occupying the antibonding orbital, but they are important intermediates in many organometallic radical reactions [6-10]. Their exceptional reactivities have intrigued much research interest, but their short lifetimes hinder a thorough study of their reactivity and electronic structure [11].

B. 19-electron complexes

19-electron organometallic complexes are formed by the reaction of 2-electron donor ligands with 17-electron radicals (Eq. 1.1) [12].

$$ML_n + L' \leftrightarrows ML_nL' \qquad \text{[Eq. 1.1]}$$

$17e^-$ ligand $19e^-$

ML_n = $CpMo(CO)_3$, $CpW(CO)_3$, $CpFe(CO)_2$, $Mn(CO)_5$, $Co(CO)_4$

L' = PR_3, $P(OR)_3$, etc.

Standard free energies of formation ($\Delta G°$) for the 19-electron complexes were obtained by measuring the equilibrium constants of Eq. 1.1. It has been found that the formation of 19-electron complexes from 17-electron complexes and a ligand can be slightly thermodynamically downhill ($\Delta G°<0$) [11, 13-15]. Some of the reactions are spontaneous (Eq. 1.2 and Eq. 1.3) [14-15].

$$[CpFe(CO)(PPh_3)CH_3]^+ + py \xleftrightarrow{K_{eq}} [CpFe(CO)(PPh_3)(CH_3)py]^+ \qquad \text{[Eq. 1.2]}$$

$$(1,3,5\text{-trimethylbenzene})W(CO)_3^+ + P(O\text{-}nBu)_3 \xleftrightarrow{K_{eq}}$$

$$(1,3,5\text{-trimethylbenzene})W(CO)_3(P(O\text{-}nBu)_3)^+ \qquad \text{[Eq. 1.3]}$$

As mentioned above, 19-electron complexes are important intermediates in many organometallic reactions. Scheme I shows a good example of such functionality. $CpMo(CO)_3L$, a 19- electron complex, acts as an intermediate in the mechanism for the photochemical disproportionation of $Cp_2Mo_2(CO)_6$ [16].

The electronic structure of 19-electron complexes hasn't been studied substantially because they are too reactive and short lived for detailed spectroscopic analyses. However the question of where the 19^{th} electron stays in the complex is still a matter of interest. An interaction of the 17-electron organometallic radical with a ligand to form a 19-electron complex is shown in Fig. 2(a). The 19^{th} electron occupies a high energy level M-L antibonding orbital. An example of such interaction is the $Mn(CO)_5Cl^-$ [12,17] complex, which is stabilized at low temperature. An ESR spectroscopy study showed that the unpaired electron in $Mn(CO)_5Cl^-$ complex does occupy the Mn-Cl π^* antibonding orbital.

It has also been suggested that in order to avoid the unpaired, 19^{th} electron occupying the high energy M-L antibonding orbitals, the ligands of some 19-electron complexes change their geometries to accommodate the additional electron in their lower energy level π^* orbitals (Fig. 2(b)) [12,16]. For example, Cp rings can slip from η^5 to η^4 (Fig. 3(a)), e.g. $CpFe(CO)_3$; CO and NO ligands can bend (Fig. 3(b)), e.g. $Cr(CO)_5CHO^-$; and phosphine or phosphite ligands can adopt a phosphoranyl radical type structure (Fig. 3(c)), e.g. $CpMo(CO)_3(P(OR)_3)$ [16]. These distortions stabilize the complexes by removing the unpaired electron from the higher energy level M-L orbital to the

lower energy level ligand orbital. Thus the 19th electron is no longer located on metal but primarily localized on the ligand. Evidence for these alternative structures were found from reactivity and electrochemical studies. For example, a bent CO ligand is found in the electrochemical reduction of $Cr(CO)_6$ (Scheme II) [18]. Electrochemical studies have shown that when many 19-electron complexes couple, they couple through the ligands, presumably because the unpaired electron is ligand localized. A classical example of two 19-electron complexes coupling through their ligands is rhodocene (Eq. 1.4**)** [16]:

$2Cp_2Rh \rightarrow$ 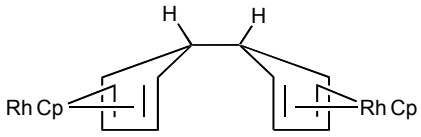

[Eq. 1.4]

C. 19-electron complexes as 18+δ systems

The phrase "19-electron complex" generally implies a 19-electron configuration at the metal center. However as discussed above, the 19th valence electron can also reside in the ligand π^* orbital rather than in the metal-ligand antibonding orbital. Therefore, it's actually an 18-electron system on the metal; the 19-electron complex becomes a misnomer. EPR studies showed that there is some delocalization of the unpaired electron from the ligand's π^* orbital onto the metal fragment, such as in the complexes of $Co(CO)_3L_2'$, $Co(CO)_3L_2''$, $Fe(CO)_3L_2'^{\cdot-}$ and $Fe(CO)_3L_2''^{\cdot-}$ (Fig. 4) [20-22]. Fig. 2(c) shows such delocalization: the unpaired electron occupies the orbital resulting from the interaction of an additional metal orbital with the ligand's π^*

orbital. Hence a new name, "18+δ", was suggested for such complexes rather than the name of "19-electron complex", because they can be described by 18-electron complexes with partial electron density contributed to the metal by delocalization of the unpaired electron from the ligand. In this nomenclature, δ is intended to indicate the amount of unpaired electronic charge delocalized onto the metal [23-26]. For complexes with no electron delocalized onto the metal from ligands, δ would be 0, and $0<\delta<1$ for those with the electron delocalized from ligands to the metal. Thus the authentic 19-electron complexes would have δ approximately equaled to 1, where the 19th electron primarily resides on the metal. For example, ESR spectroscopy has showed that $\delta=0.015$ in the $Co(CO)_3L_2$ complex and $\delta=0.09$ in the $Fe(CO)_3L'^{-}_2$ complex (Fig. 4). The small value of δ indicates that the 19th electron is primarily localized on the ligand in these two complexes with a small delocalization on to the metal [27].

Experimental chemists have been trying different strategies to synthesize 18+δ complexes to study the structures and properties of those complexes. However they are too reactive to last long for detailed studies; so far only limited number of 18+δ complexes have been generated successfully, and the 19-electron complexes as 18+δ systems still remain as a great interest. More recently, computational methods have been introduced to help study the possible structures of 18+δ systems and locate the 19th electron. Computational methods are quick and convenient compared to experimental methods. The accuracy of calculated results on organometallic complexes using ab initio methods, such as equilibrium geometries, reaction energies,

bond energies and vibrational frequencies, is often comparable and sometimes even superior to experimental data. Some examples are given in Table 1 and Table 2 [5]. The results agree well with reported experimental data. Such theoretical calculations also predict the properties for unavailable molecules. Computational methods could be a reliable and alternative way to help understand available complexes and complexes that are difficult to synthesize experimentally. Chapter II explains one such computational method, namely Density Functional Theory (DFT), in detail, and some other important concepts of computational methods, such as basis sets.

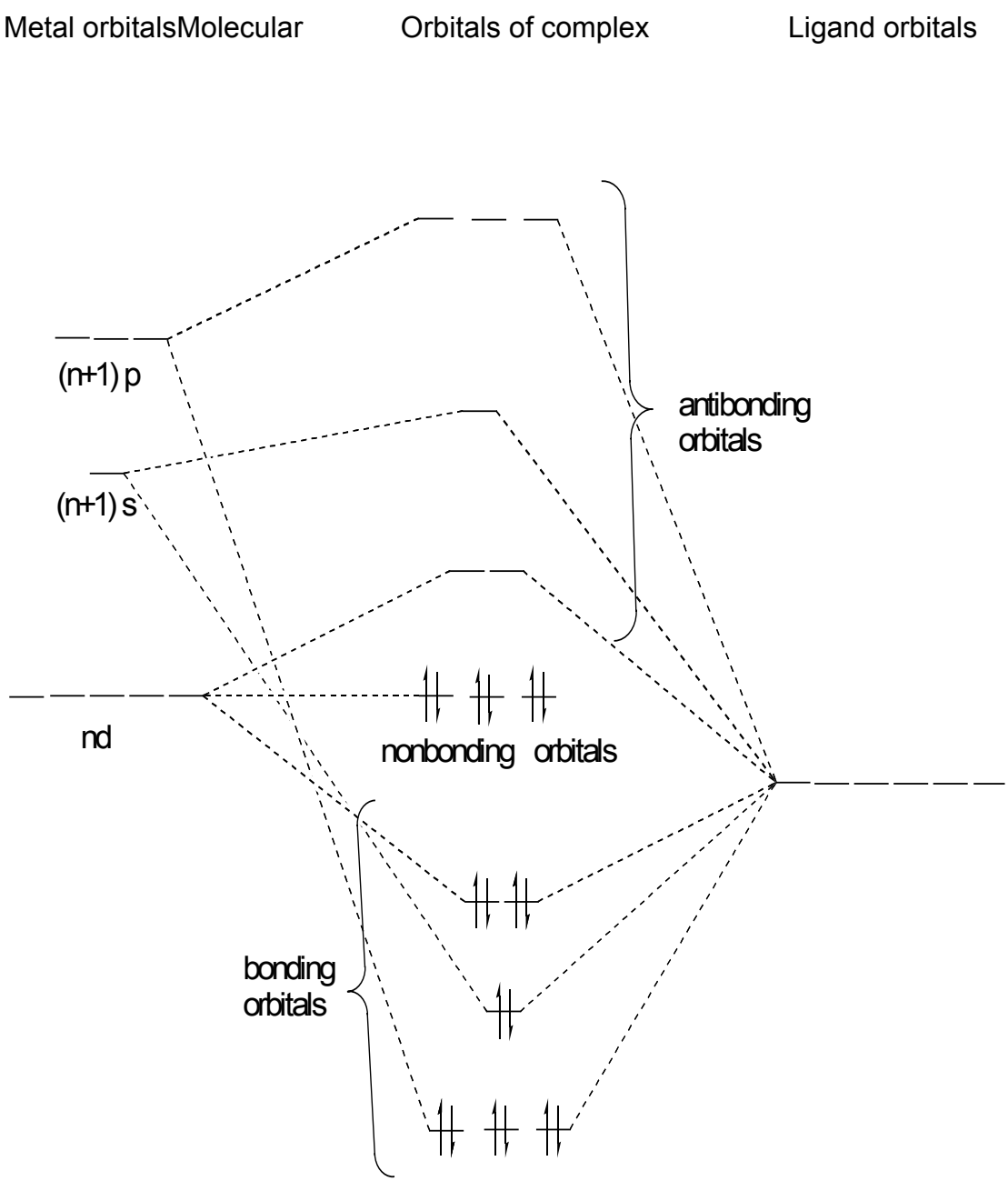

Figure 1. Molecular orbital diagram of an octahedral complex:
A transition metal organometallic complex with six ligands

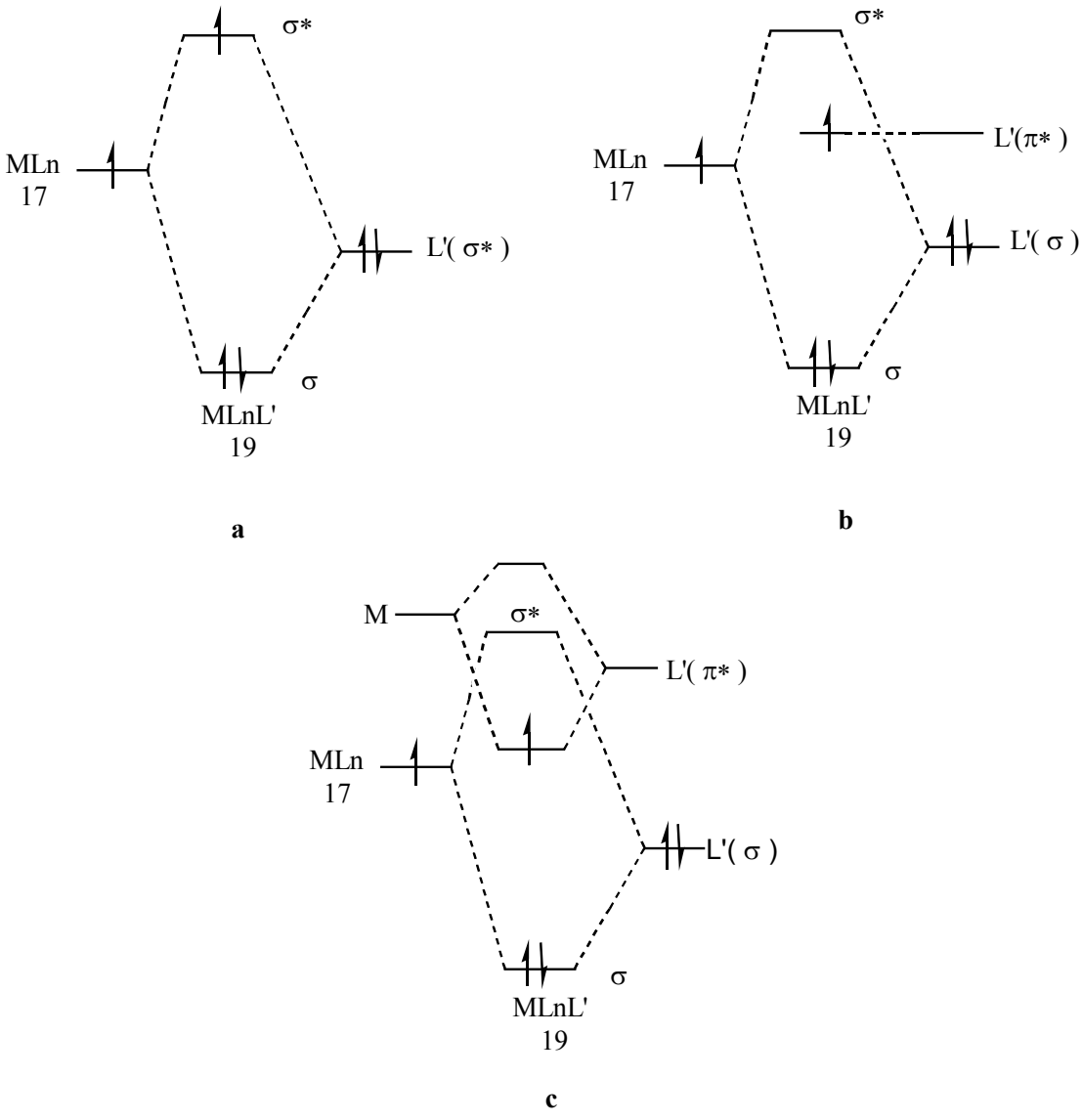

Figure 2. A simplified molecular orbital scheme showing the interaction of the singly occupied orbital on a 17-electron organometallic radical with a ligand orbital to form molecular orbitals of a 19-electron complex.
(a) The 19th electron occupies a M-L antibonding orbital σ*.
(b) The 19th electron occupies the lower-energy ligand π* orbital.
(c) An additional metal orbital is interacting with the ligand π* orbital, leading to the 19th electron delocalized onto the metal.

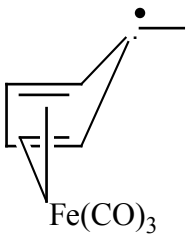

a

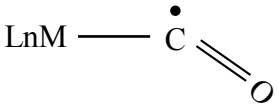

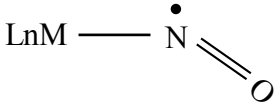

b

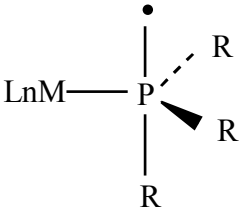

c

Figure 3. Alternative structures for 19-electron complexes in which the unpaired, 19th electron is localized on ligand:
(a) A $\eta^5 \rightarrow \eta^4$ Cp ring slippage.
(b) A bent CO and NO ligand.
(c) A trigonalpyramidal phosphoranyl radical type structure.

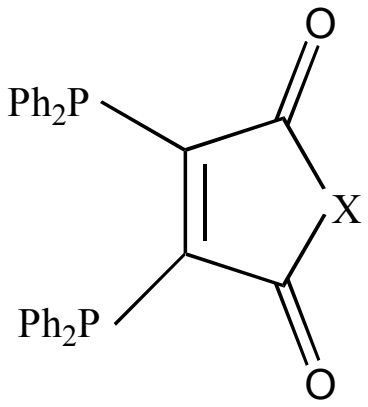

L_2': X=O; L_2'': X=CH_2

Figure 4. Ligand structure in $Co(CO)_3L_2$', $Co(CO)_3L_2$'', $Fe(CO)_3L_2$'$^-$ and $Fe(CO)_3L_2$''$^-$

$$Cp_2Mo_2(CO)_6 + L \xrightarrow{h\upsilon} CpMo(CO)_3L^+ + CpMo(CO)_3^-$$

Overall Reaction (1)

$$Cp_2Mo_2(CO)_6 \xleftrightarrow{h\upsilon} 2\ CpMo(CO)_3$$ Initiation (2)

$$CpMo(CO)_3 + L \xleftrightarrow{K_{eq}} CpMo(CO)_3L$$ Propagation (3)

$17e^-$ $19e^-$

$$CpMo(CO)_3L + Cp_2Mo_2(CO)_6 \rightarrow CpMo(CO)_3L^+ + Cp_2Mo_2(CO)_6^-$$ (4)

$18e^-$

$$Cp_2Mo_2(CO)_6^- \rightarrow CpMo(CO)_3^- + CpMo(CO)_3$$ (5)

$18e^-$ $17e^-$

$$CpMo(CO)_3L + CpMo(CO)_3 \rightarrow CpMo(CO)_3L^+ + CpMo(CO)_3^-$$

$19e^-$ $17e^-$ $18e^-$ $18e^-$ Termination (6)

Scheme I Mechanism for the Photochemical Disproportionation of $Cp_2Mo_2(CO)_6$

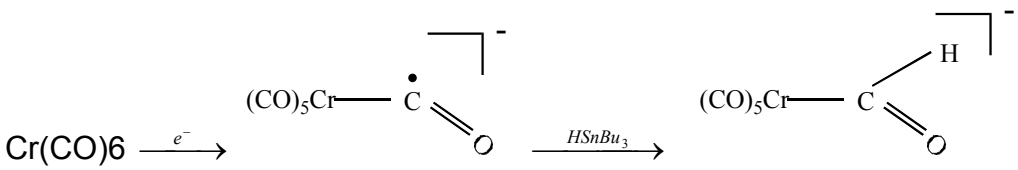

18e 19e$^-$ complex but actually 18e$^-$ on the metal +$SnBu_3$

Scheme II A reaction that suggests some 19-electron complexes may have bent CO ligands

Table 1. Calculated and experimental bond lengths (Å) and angles (°) of Oxo and Nitrido complexes [5]

MXLn	M-X		$M-L_{eq}$		Angle ($X-M-L_{eq}$)	
	HF	Exp.	HF	Exp.	HF	Exp.
$MoOF_4$	1.62	1.65	1.835	1.836	105.5	103.8
$MoOCl_4$	1.614	1.658	2.311	2.279	104.6	1028
WOF_4	1.644	1.666	1.834	1.847	105.2	104.8
$WOCl_4$	1.636	1.684	2.311	2.280	104.3	102.6
$ReOF_4$	1.614	1.609	1.834	1.823	107.8	108.8
$ReOCl_4$	1.611	1.663	2.306	2.270	106.0	105.5
$OsOF_4$	1.602	1.624	1.840	1.835	110.3	109.3
$OsOCl_4$	1.604	1.663	2.299	2.258	107.9	108.3
$MoNF_3$	1.585		1.835		104.5	
$MoNF_4^-$	1.596	1.83	1.917	1.730	103.7	99.0
$MoNF_5^{2-}$	1.634		1.952		95.7	
$MoNCl_3$	1.585		2.283		104.4	
$MoNCl_4^-$	1.586	1.66	2.409	2.345	101.9	101.5
$MoNCl_5^{2-}$	1.603		2.463		93.6	
WNF_3	1.623		1.847		105.8	
WNF_4^-	1.636		1.906		104.8	
WNF_5^{2-}	1.675		1.938		97.2	
$WNCl_3$	1.622		2.276		105.4	
$WNCl_4^-$	1.624		2.399		102.9	
$WNCl_2F_2^-$	1.632	2.23	2.428	2.31(Cl)	103.9	81.6
			1.884	1.66(F)	103.9	129.1
$WNCl_5^{2-}$	1.642		2.451		94.9	
$ReNF_4^-$	1.602		1.910		106.0	
$ReNF_4$	1.59		1.926		101.1	
$ReNCl_4^-$	1.595	1.619	2.394	2.322	103.0	103.5
$ReNCl_4$	1.597	1.58	2.315	2.320	101.6	100.0
$OsNF_4^-$	1.587		1.917		107.5	
$OsNF_5^{2-}$	1.618		1.972		96.5	
$OsNCl_4^-$	1.585	1.60	2.381	2.310	103.7	104.6
$OsNCl_5^{2-}$	1.602	1.61	2.452	2.360	93.6	96.2

Table 2. Calculated and experimental vibrational frequencies (cm^{-1}) [5] (Continued)

Symmetry	$MoOF_4$		$MoOCl_4$		WOF_4		$WOCl_4$	
	HF	Exp.	HF	Exp.	HF	Exp.	HF	Exp.
A1	1234	1049	1207	1017	1211	1055	1196	1032
	801	714	411		807	733	408	400
	283	264	181		271	248	167	
B2	681		291		709		302	
	105		44		115		46	
B1	350		235		359		240	
E	808	720	409	395	782	698	384	380
	337	294	274		337	298	281	260
	254	236	146		262	236	157	

Symmetry	$ReOF_4$		$ReOCl_4$		$OsOF_4$		$OsOCl_4$	
	HF	Exp.	HF	Exp.	HF	Exp.	HF	Exp.
A1	1255	1077	1229	1040	1280	1079	1247	1032
	808	714	395	402	803		396	
	266		164		264		165	
B2	724		310		741		337	
	109		56		106		60	
B1	331		225		320		221	
E	789	700	382	392	800	685	402	395
	343		283		367	319	288	
	276		174		264		191	

Table 2. Calculated and experimental vibrational frequencies (cm^{-1}) [5] (continued)

Symmetry	$MoNF_4^-$ HF	$MoNF_4^-$ Exp.	$MoNCl_4^-$ HF	$MoNCl_4^-$ Exp.	$WNCl_4^-$ HF	$WNCl_4^-$ Exp.	$ReNCl_4^-$ HF	$ReNCl_4^-$ Exp.
A1	1300	969	1278	1054	1260	1036	1315	1085
	679	620	347	355	351	336	344	358
	272		166		155		150	
B2	573		272		272			286
	137		69		69			69
B1	296		197		197			182
E	679	600	354	344	311	303	336	341
	368		292	278	292	233	291	
	230		146		146		155	

Symmetry	$OsNCl_4^-$ HF	$OsNCl_4^-$ Exp.	$OsNCl_5^{2-}$ HF	$OsNCl_5^{2-}$ Exp.
A1	1345	1123	1306	1084
	348	358	312	384
	147	184	200	324
			159	184
B2	309	352	285	334
	66	149	113	169
B1	178	174	146	181
E	354	365	309	336
	290	271	281	264
	165	132	155	172
			117	146

CHAPTER REFERENCES

1. Miessler G.L., *Inorganic Chemistry*, 2nd Edition, 1998
2. Collman J.P., Hegedus L.S., Norton J.R. and Finke R.G., *Principles and Applications of Organotransition Metal Chemistry,* 1987
3. Herrinton T.R., Brown T.L., *J. Am. Chem. Soc.* 1985, *107*, 5700
4. Tyler D.R., *Prog. Inorg. Chem*. 1988, *36*, 125
5. Lipkowitz K.B., Boyd D.B., *Reviews in computational chemistry*, 1996, *8*, 63
6. Astruc D., *Chem. Rev*. 1988, *88*, 1189
7. Tyler D.R., In *Organometallic Radical Processes*; Trogler W.C., Ed.; Elsevier: New York, 1990, 338
8. Tyler D.R., Mao F., *Coord. Chem. Rev*. 1990, *97*, 119
9. Geiger W.E., *Acc. Chem. Res*. 1995, *28*, 351
10. Braden D.A., Tyler D.R., *J. Am. Chem. Soc*. 1998, *120*, 942
11. Castellani M.P., Tyler D.R., *Organometallics* 1989, *8*, 2113
12. Lionel T., Morton J.R., Preston K.F., *Chem. Phys. Lett*. 1981, *81*, 17
13. Philbin C.E., Granatir C.A. and Tyler D.R., *Inorg. Chem*. 1986, *25*, 4806
14. Therien M., Trogler W.C., *J. Am. Chem. Soc.* 1987, *109*, 5127
15. Zhang Y., Gosser D.K., Rieger P.H. and Sweigart D.A., *J. Am. Chem. Soc*. 1991, *113*, 4062
16. Tyler D.R., *Acc. Chem. Res*. 1991, *24*, 325

17. Peake B.M., Symons M.C.R. and Wyatt J.L., *J. Chem. Soc*., *Dalton Trans*. 1983, 1171

18. Narayanan B.A., Kochi J.K., *J. Organomet. Chem*. 1984, *272*, C49

19. Geiger W.E., Gennett T., Lane G.A., Slazer A. and Rheingold A.L., *Organometallics* 1986, *5*, 1352

20. Weil J.A., Bolton J.R., Wertz J.E., *Electron Paramagnetic Resonance*; Wiley: New York, 1994

21. Duffy N.I.W., Nelson R.R., Richmond M.G., Rieger A.L., *Inorg. Chem*. 1998, *37*, 4849

22. Braden D.A., Tyler D.R., *Organometallics*, 2000, *19*, 3762

23. Olbrich-Deussner B., Kaim W., *J. Organomet. Chem.* 1988, *340,* 71

24. Brown T.L., *In Organometallic Radical Processes*; Trogler W.C., Ed.; Elsevier: New York, 1990, *67*

25. Mao F., Tyler D.R., Bruce M.R.M., Bruce A.E., Rieger A.L. and Rieger P.H., *J. Am. Chem. Soc.* 1992, *114*, 6418

26. Schut D.M., Tyler D.R., Rieger P.H., *J. Am. Chem. Soc.* 1995, *117*, 8939

27. Mao F., Tyler D.R., Rieger A.L., Rieger P.H., *J. Chem. Soc*., Faraday Trans., accepted for publication.

CHAPTER II

THEORETICAL METHODS

SECTION I DENSITY FUNCTIONAL THEORY

A. Introduction

Density Functional Theory (DFT) is one member of electronic structure methods; the other two methods are semi-empirical methods and ab initio methods. The DFT method distinguishes itself from the other two by expressing its results in terms of electron density, ρ. The basis of DFT theory was proved by Hohenberg and Kohn [1] about three decades ago. It states that the ground-state electronic energy is determined completely by the electron density, which means that there exists a one-to-one relationship between the electron density and the energy of a system. The goal of DFT methods is to design the functional which connects the energy with the electron density, ρ [2].

In the past few years, DFT methods have gained steady popularity and have been applied extensively to the problems, which were previously solved by ab initio Hartree-Fock methods. In practice, a DFT calculation involves similar efforts to those required for an ab initio Hartree-Fock (HF) calculation, whose computational efforts both scale as N^4 (N stands for the number of basis functions). Also DFT methods are one-dimensional just as HF methods, which means that increasing the size of the basis set allows for better results. Despite the similarities between DFT and HF methods, DFT methods can

possibly achieve greater accuracy than HF methods at almost the same cost. Such advantage is due to the fact that DFT methods include some effects of electron correlation, ignored in HF calculation, at a much lower computational cost than traditional correlated methods do, such as MP2 and QCISD. In HF, electron correlation is only considered in an average field, thus leading to its insufficient accuracy in some systems where electron correlation is essential. The advantage of DFT methods to traditional methods is more obvious when used on larger molecular systems and heavy-atom molecules.

However DFT is a comparatively new method to the field of computational chemistry. It only has about a 30-year-history so far, while the conventional quantum methods have been used for 70 years. Various new functionals and methodologies need to be developed. Currently, there is no known systematic way to judge the quality of new functionals, and the calibration system for DFT methods is less developed. Therefore, certain cautions should be taken to judge the performance of DFT methods. The results need to be compared with experimental data or higher level ab initio methods to evaluate the calculation quality.

B. Theory behind DFT

The DFT approach is based on a one-to-one correspondence between the energy of the system and the electron density ρ by designing a functional to connect them. The DFT functional divides the electronic energy into several terms:

$$E = E^T + E^V + E^J + E^{XC} \qquad \text{[Eq. 2.1]}$$

E^T - Kinetic energy term, arising from the motions of electrons.

E^V - Potential energy term, arising from nuclear-electron attraction and nuclear-nuclear repulsion.

E^J - Electron-electron repulsion term, also described as the Coulomb self-interaction of the electron density.

E^{XC} - Exchange-correlation term, describing the remaining part of the electron-electron interaction, which includes the exchange energy arising from the antisymmetry of the quantum mechanical wavefunction and dynamic correlation in the motions of the individual electrons.

All the terms above are functions of the electron density, ρ, except for nuclear - nuclear repulsion. Terms E^V and E^J are expressed as follows:

$$E^V = \sum_a \int Z_a \rho(r) (|R_a - r|)^{-1} dr \qquad \text{[Eq. 2.2]}$$

$$E^J = \frac{1}{2} \int \int \rho(\vec{r}_1)(\Delta r_{12})^{-1} \rho(\vec{r}_2) d\vec{r}_1 d\vec{r}_2 \qquad \text{[Eq. 2.3]}$$

E^{XC} is a unique term. It replaces the exact exchange for a single determinant in HF with a more general expression, the exchange-correlation functional E^{XC}, which includes the electron correlation to account for both exchange energy and the electron correlation that is omitted in HF theory (E^c=0). The E^{XC} term is usually separated into two parts, the exchange part, E^x, and the correlation part, E^c, corresponding to same-spin and mixed-spin interactions, respectively.

$$E^{XC}(\rho) = E^x(\rho) + E^C(\rho) \qquad \text{[Eq. 2.4]}$$

Again the above three terms are all functionals of electron density, ρ. Both the exchange part E^x and the correlation part E^c can be of two distinct types: local functionals, which depends only on the electron density, ρ, and gradient-

corrected functionals, which depends on both the electron density, ρ, and its gradient, $\nabla\rho$, respectively.

Let's look at them separately. The local density functional assumes that the density can be locally treated as a uniform electron gas. The local exchange functional is always defined as follows:

$$E^{X}_{LDA}[\rho] = -\frac{3}{2}\left(\frac{3}{4\pi}\right)^{1/3}\int \rho^{4/3}\, d^3\vec{r} \qquad \text{[Eq. 2.5]}$$

The local correlation functional has the form

$$E^{C}_{LDA}[\rho] = \int \rho_1(\vec{r}_1)\,\varepsilon_c[\rho^{\alpha}_1(\vec{r}_1)\,\rho^{\beta}_1(\vec{r}_1)]\, d\vec{r}_1 \qquad \text{[Eq. 2.6]}$$

where $\varepsilon_c[\rho^{\alpha}_1, \rho^{\beta}_1]$ represents the correlation energy per electron in a gas with the spin densities, ρ^{α}_1 and ρ^{β}_1. The specific correlation energy is not known analytically. However, approximations of increasing accuracy have been developed [3,4]. Recently Vosko, Wilk and Nusair (VWN) constructed the results from Monte Carlo methods to make them suitable for the DFT calculations [5].

The local density approximation (LDA) agrees very well with experimental results for bond lengths, bond angles, vibrational frequencies and charge densities [6,7]. But it is weak in describing thermochemical properties. In general, the LDA underestimates the exchange energy by ~ 10%, and the correlation energy is furthermore overestimated, often by a factor of 2. As a consequence, bond energies, in particular, deviate greatly from experiments [8]. For example, the O_2 molecule was calculated by LDA to be overbound by a huge 55 kcal/mol, with a deviation of 20-30 kcal/mol.

The gadient-corrected functional is an improvement over LDA. It considers the density as a non-uniform electron gas, including both the values of the electron spin densities and their gradients. It is also referred to as the generalized gradient approximation (GGA) or non-local methods. B88 is a widely used gradient-corrected functional proposed by Becke [9]. Eq. 2.9 shows the functional expression

$E^{X}_{B88} = E^{X}_{LDA} + \Delta\varepsilon^{X}_{B88}$ [Eq. 2.7]

$\Delta\varepsilon^{X}_{B88} = -\beta\rho^{1/3} \frac{x^2}{1+6x\beta\sinh^{-1}x}$

$\chi = \frac{|\nabla\rho|}{\rho^{4/3}}$, and the β parameter is determined by fitting to known atomic data.

Various other gradient-corrected correlation functionals have been proposed. One of the most popular functionals is presented by Lee, Yang, and Parr [10], LYP, a second-order gradient expansion. It has the form

$E^{C}_{LYP} = -a \frac{\gamma}{(1+d\rho^{-1/3})} - ab \frac{e^{-c\rho^{-1/3}}\gamma}{9(1+d\rho^{-1/3})\rho^{8/3}} \times$

$[18(2^{2/3})C_F(\rho_\alpha^{8/3} + \rho_\beta^{8/3}) - 18\,\rho\, t_W + \rho_\alpha(2t_W^\alpha + \nabla^2\rho_\alpha) + \rho_\beta(2t_W^\alpha + \nabla^2\rho_\beta)$

$\gamma = 2[1-\frac{\rho_\alpha^2+\rho_\beta^2}{\rho^2}]$ and $t_W^\sigma = \frac{1}{8}(\frac{|\nabla\rho_\sigma|^2}{\rho^\sigma} - \nabla^2\rho_{\sigma\sigma})$ [Eq. 2.8]

Parameters *a,b,c* and *d* are obtained by Colle and Salvetti [11] from a fit to the helium atom.

The GGA yields good thermochemical results; an average error on the order of 6 kcal/mol is achieved in standard thermochemical tests [12]. It also treats the energy and structure of hydrogen-bonded system with quality [13].

However the GGA fails in the calculation of van der Waals interactions [14,15].

C. Pure and hybrid DFT methods

Pure DFT methods are defined as pairing an exchange functional with a correlation functional. For example, BLYP is a well-known pure DFT method, which pairs Becke's gradient-corrected exchange functional with the gradient-corrected correlation functional of Lee, Yang and Parr (LYP). Hybrid DFT methods are a counterpart of pure DFT methods. It makes an exact connection between the exchange-correlation energy and the corresponding potential, which connects the non-interacting reference and the actual system.

Hybrid DFT methods include hybrid functionals. Becke has developed several hybrid functionals that include a mixture of Hartree-Fock exchange with DFT exchange-correlation functionals. The exchange functional is defined as a linear combination of Hartree-Fock, local, and gradient-corrected exchange terms; then this exchange functional is combined with a local and/or gradient-corrected correlation functional. The hybrid exchange-correlation, E^{XC} term is defined as

$$E_{hybrid}^{XC} = c_{HF}E_{HF}^{X} + c_{DFT}E_{DFT}^{XC} \qquad \text{[Eq. 2.9]}$$

Where *c*'s are constants

Hartree-Fock theory includes an exchange term in its own definition (shown as $c_{HF}E_{HF}^{X}$ in Eq. 2.9), which gives the exact exchange energy when the electrons' interaction is zero. The best known of these hybrid

functionals are Becke's three-parameter functionals, such as B3LYP, B3P86 and B3PW91. The B3LYP functional has the following expression [16]

$$E_{B3LYP}^{XC} = E_{LDA}^{X} + a\,(E_{HF}^{X} - E_{LDA}^{X}) + b\Delta E_{B88}^{X} + E_{VWN3}^{C} + c\,(E_{LYP}^{C} - E_{VWN3}^{C}) \quad \text{[Eq. 2.10]}$$

The parameters *a, b* and *c* were determined by Becke by fitting to the atomization energies, ionization potentials, proton affinities and first-row atomic energies in the G1 molecule set [17-19]. The values are *a*=0.20, *b*=0.72 and *c*=0.81. The parameter *a* allows any combination mixture of HF and LDA local exchange, while the Becke's gradient correction to LDA exchange is also included by the term $b\Delta E_{B88}^{X}$. For correlation energy, the VWN3 local correlation functional is used and corrected by LYP correlation functional via parameter *c*.

Pure DFT methods often do not do well for transition states of organic molecules while the hybrid methods seem to handle the problem very well.

SECTION II BASIS SETS

A. Introduction

All theoretical calculations use a basis set expansion to express the unknown molecular orbital (MO) in terms of a set of known functions to solve the Schrödinger equation. A basis set is a mathematical description of the orbitals within a system (which in turn combine to approximate the total electronic wavefunction) to perform the theoretical calculation. The molecular orbitals Ψ_i can be expressed as a linear combination of N nuclear-centered basis functions (also referred to as atomic orbitals, AO) ϕ_μ (μ=1,2,…,N),

$$\Psi_i = \sum_{\mu}^{N} c_{\mu i} \phi_\mu \qquad \text{[Eq. 2.13]}$$

Eq. 2.13 can be an exact relationship if the basis set is complete, which means that an infinite number of basis functions are being used. This is entirely impossible in actual calculations. The computational effort of ab initio methods scale as at least N^4 (N= the number of basis functions). Larger basis sets give more accurate approximations of the orbitals but require greater computational efforts, and smaller basis sets lead to poorer representations at lower expense. It implies that some compromises need to be made between computational cost and accuracy. It is important to make the basis sets as small as possible while not sacrificing the accuracy in calculations. The type of basis function also influences the accuracy, which should be physically meaningful and easy to calculate all the required integrals.

B. Characteristics of Basis Sets

Basis sets assign a group of basis functions to each atom in the molecular system to approximate the orbitals. There are two types of basis functions: Slater Type Orbitals (STO) [20] and Gaussian Type Orbitals (GTO) [21]. Comparing these two, GTOs are less satisfactory than STOs because GTOs represent improper behavior near the nucleus. However STOs are much more complicated in numerical computatioins, which make them unsuitable for practical calculations, while all integrals in the computations of GTOs can be evaluated explicitly.

Therefore a procedure that has come into wide use is to fit a STO to a linear combination of primitive Gaussian functions, which simplifies the numerical works of STO by still evaluating integrals only with primitive Gaussian functions but improves the behavior of GTOs in the meantime.

$$\phi_\mu = \sum_p d_{\mu p} g_p \qquad \text{[Eq. 2.14]}$$

where $d_{\mu p}$'s are fixed constants and g_p's are primitives.

Basis functions, which have the above form, are referred to as contracted functions. A basis function consisting only of a single Gaussian function is defined as uncontracted. In the next section, more detail of the types of basis sets will be discussed.

C. General Types

i. Minimal Basis Sets

Minimal basis sets use fixed-size atomic-type orbitals and only employ the minimum number of functions to contain all the electrons in the neutral atoms.

For example,

Li - Ne: 1s, 2s, $2p_x$, $2p_y$, $2p_z$

STO-3G is a minimal basis set. A minimal basis set only contains a single valence function of each symmetry type; therefore it's unable to expand and contract in response to different molecular environments. For example, Li contains 3 electrons and F contains 9 electrons but the number of basis functions assigned to them is both 5. It's likely to give a poor description, especially with anisotropic molecules and polar molecules.

ii. Split Valence Basis Sets

Split valence basis sets allow for more than one single basis function for each valence orbital. For example,

Li–Ne: 1s, 2s, 2s', $2p_x$, $2p_x$', $2p_y$, $2p_y$', $2p_z$, $2p_z$'

where the prime and unprimed orbitals differ in size. 3-21G is an often seen split-valence basis set. 6-31G is a larger split-valence basis set and 6-311G is a triply split-valence basis set.

The use of additional basis functions for valence s, p and/or d orbital in split-valence basis sets has helped in describing anisotropic and polar molecules.

iii. Polarized and Diffuse Basis Sets

The basis sets described above are comprised of functions centered at the nuclear positions and are suitable for molecules whose electrons are tightly held to the nuclear center. Additional adjustments need to be made to add more flexibility to the basis sets to account for exceptional molecules.

Polarization functions:

By adding orbitals with higher angular momentum above what is required for the ground state to each atom allow orbital to change shape. This change helps to work with polar molecules, small strained rings molecules, etc. Polarization functions are important in most bonding description in many molecules. 6-31G(d), also known as 6-31G*, is a common polarized basis set, which means adding additional d functions to heavy atoms (non-H atoms). Another popular polarized basis set is 6-31G(d,p), which also referred to as 6-31G**. It not only adds an extra d function to non-H atoms but also adds an additional p function to H and He.

Diffuse functions:

Diffuse functions are normally s- and p- functions to allow orbitals to occupy larger region of space. Basis sets with diffuse functions are essential for systems where the electron density is far away from the nucleus, such as anions, molecules with lone pairs or excited states. Diffuse functions help greatly to calculate electron affinities, proton affinities and inversion barriers.

Diffuse functions are denoted as "+". For example, in 6-31++G (d) or 6-31++G* notation, the first + means adding a set of diffuse s- and p- function in addition to a d polarized function to heavy atoms and the second + indicates to adding a diffuse s- function to H and He.

iv. Effective Core Potentials and Associated Basis Sets

The elements in the third row or higher row in the periodic table are more difficult to model than the elements in the lower rows. There are two reasons for this:

1. Large number of core electrons in those elements.

2. Relativistic effects in those elements are often non-negligible

Therefore basis sets for systems with those heavy elements are often be handled somewhat differently. The core electrons need to be treated differently from valence shell electrons to account for the relativistic effects and the effects of core electrons on the valence shell electrons. The problem is solved by introducing an Effective Core Potential (ECP) (also referred to as "pseudopotential") to represent all the core electrons [22,23]. The ECPs include all electron shells except for the outermost one, valence shell. The core electrons are replaced by a linear combination of Gaussian functions while the valence electrons are treated explicitly with proper basis sets.

In detail, there are four major steps in designing ECP type basis sets. First a good quality all-electron wave function is generated for the atom. Then the valence orbitals are replaced by a set of pseudo-orbitals. This set of pseudo-orbitals is designed to be nodeless so that the outer part will behave correctly but will not have nodal structure in the core region to be orthogonal to the core orbitals. Then the core electrons are replaced by a numerical potential so that the solution to the Schrödinger equation produces valence orbitals matching the pseudo-orbitals. Lastly, this numerical potential is fitted to a suitable set of Gaussian functions, Eq. 2.15 [24]

$$U_{ECP}(r) = \sum_i a_i r^{n_i} e^{-\alpha_i r^2} \qquad \text{[Eq. 2.15]}$$

The parameters a_i, n_i and α_i depend on the angular momentum (s-, p-, d-, etc.).

The LANL2DZ basis set is one such ECP. This basis set uses the valence double-ζ (DZ) basis set on light elements and effective core potentials plus DZ on heavy elements [25]. The SBKJC-21G (The Stevens-Basch-Krauss-Jansien-Cundari set) is another example of ECPs with the associated basis sets ([4211/4211/411]) [26]. In these effective core potentials, the core consists of all but the outermost electrons. The performance of most ECPs agrees with the experimental results [27].

D. Natural Bond Orbital

Natural bond orbital (NBO) analysis was originated as a technique for studying hybridization and covalency effects in polyatomic wave functions [28]. It is useful to understand the bonding in molecules. The NBO method extracts the information in the first-order density matrix of the ab initio calculations. Then develops a unique set of atomic hybrids and bond orbitals for a given molecule, thereby leading to “Lewis structure” which is easy to understand.

The general procedure consists of a sequence of transformations from the input basis set $\{\chi_i\}$ to various localized basis sets (natural atomic orbitals (NAOs), hybrid orbitals (NHOs), bond orbitals (NBOs), and localized molecular orbitals (NLMOs)) [29].

Input basis → NAOs → NHOs → NBOs → NLMOs

The NLMOs may be subsequently transformed to delocalized natural orbitals (NOs) or molecular orbitals (MOs). The above steps are automated by the NBO computer programs [30].

A NAO is a valence-shell atomic orbital whose derivation involves diagonalizing the localized block of the full density matrix of a given molecule associated with input basis function $\chi_i(A)$ on that atom. In a polyatomic molecule, the NAOs mostly retain one-center character, and thus are optimal for describing the molecular electron density around each atomic center. The resulting atomic charge on each atom corresponds to natural atomic charge.

The NBO is formed from NHOs. For a localized σ-bond between atoms A and B, the NBO is:

$$\sigma_{AB} = c_A h_A + c_B h_B \qquad \text{[Eq. 2.16]}$$

where h_A and h_B are the natural hybrids centered on atoms A and B. NBOs closely correspond to the picture of localized bonds and lone pairs as basic units of molecular structure, so that it is possible to conveniently interpret ab initio wavefunctions in terms of the classical Lewis structure concepts by transforming these functions to NBO form. The results of NBO analysis agree well with ab initio calculations.

E. Computational Methods

In this work, all the molecular structures were optimized and characterized by using hybrid DFT method, B3LYP. The standard 6-31G(d) basis set was used for elements Br, H, P and O. For Co and Re, the SBKJC-21G relativistic effective core potential and its associated basis set ([4211/4211/411]) was used. All the computations were carried out with the Gaussian-98 program package [31]. Natural atomic charges were obtained from NBO analysis.

CHAPTER REFERENCES

1. Hohenberg P., Kohn W., *Phys. Rev*. 1964, *136*, B864
2. Parr R.G., Yang W., *Density Functional Theory*, Oxford University Press, 1989
3. Gunnarsson O., Lundquist I., *Phys. Rev*. 1976, *B13,* 4274
4. von Barth U., Hedin L., *Phys. Rev.* 1979, *A20*, 1693
5. Vosko S.J., Wilk L. and Nusair M., Can. *J. Phys.* 1980,*58*, 1200
6. Andzelm J., Wimmer E., *J. Chem. Phys.* 1992, *96*, 1280
7. Johnson B.G., Gill P.M.W. and Pople J.A., *J. Chem. Phys*. 1993, *98*, 5612
8. Becke A.D., *Phys. Rev. A* 1986, *33*, 2786
9. Becke A.D., *Phys. Rev.,* 1988, *38*, 3098
10. Lee C., Yang W. and Parr R.G., *Phys. Rev. B.* 1988, *37*, 785
11. Colle R., Salvetti O., *J. Chem. Phys.* 1983, *79*, 1404 and references therein
12. Becke A.D., *J. Chem. Phys.* 1992, *96*, 2155; 1992, *97*, 9173
13. Sim F., St-Amant A., Papai I. And Salahub D.R., *J. Am. Chem. Soc*. 1992, *114*, 4391
14. Kristyan S., Pulay P., *Chem. Phys. Lett.* 1994, *229*, 175
15. Perez-Jorda J.M., Becke A.D., *Chem. Phys. Lett*. 1995, *233*, 134
16. Foresman J.B., *Exploring chemistry with electronic structure methods*, 2nd edition, Gaussian, Inc, 1996
17. Becke A.D., *J. Chem. Phys*. 1993,*98* 5648

18. Pople J.A., Head-Gordon M, Fox D.J., Raghavachari K. and Curtiss L.A, *J. Chem. Phys*. 1989, *90*, 5622
19. Curtiss L.A., Raghavachari K., Trucks G.W. and Pople J.A., *J. Chem. Phys*. 1990, *93*, 2537
20. Slater J.C., *Phys. Rev*. 1930, *36,* 57
21. Boys S.F., *Proc. Roy. Soc. (London)*, 1950, *A200*, 542
22. Frenking G., Antes I., Böhme M., Dapprioh S., Ehlers A.W., Jonas V., Nauhaus A., Otto M., Stegmann R., Veldkamp A. and Vyboishchikov S.F., *Rev. Comput. Chem.* 1996*, 8*, 63
23. Cundari T.R., Benson M.T., Lutz M.L. and Sommerer S.O., *Rev. Comput. Chem*. 1996, *8*, 145
24. Jensen F., *Introduction to Computational Chemistry*, Wiley, 1999
25. Hay P.J., Wadt W.R., *J. Chem. Phys*. 1982, *77*, 3654
26. Stevens W., Krauss J.M., Basch H. and Jasien P.G., *Can. J. Chem*. 1992, *70,* 612
27. Dyall K., *J. Chem. Phys*. 1991, *96*, 1210
28. Foster, J. P., Weinhold, F., J. Am. Chem. Soc., 1980, 102, 7211-7218
29. Reed, A.E., Curtiss, L.A. and Weinhold F., Chem. Rev., 1988, 899-926
30. Reed, A.E., Weinhold, F., F. QCPE Bull., 1985, 5, 141
31. Gaussian 98, Revision A.9, Frisch, M.J., Trucks, G.W., Schlegel, H. B., Scuseria, G.E., Robb, M.A., Cheeseman, J.R., Zakrzewski, V.G., Montgomery, J.A., Stratmann, Jr.,R.E., Burant, J.C., Dapprich S., Millam, J.M., Daniels, A.D., Kudin, K.N., Strain, M.C., Farkas, O., Tomasi, J., Barone, V., Cossi, M., Cammi, R., Bennucci, B., Pomelli, C., Adamo, C., Clifford, S., Ochterski, J., Petersson, G.A., Ayala, P. Y.,

Cui, Q., Morokuma, K., Malick, D.K., Rubuck, A.D., Raghavachari, K., Foresman, J.B., Cioslowski, J.J., Ortiz, V.A., Baboul, G., Stefanov, B. B., Liu, G., Liashenko, A., Piskorz, P., Komaromi, I., Gomperts, R., Martin, R.L., Fox, D.J., Keith, T., Al-Laham, M.A., Peng, C.Y., Nanayakkara, A., Challacombe,M., P. Gill, M.W., Johnson, B., Chen, W., Wong, M.W., Andres, J.L., Gonzalez, C., Head-Gordon, M., Replogle, E. S. and Pople, J. A. Gaussian, Inc., Pittsburgh PA, 1998.

CHAPTER III

A B3LYP STUDY OF 18+δ ORGANOMETALLIC COMPLEXES

A. Introduction

The structures and properties of 18+δ organometallic systems are of great interest to chemists, but those complexes are too reactive to remain stable and therefore difficult to synthesize in the lab, which requires special strategies and great efforts. Computational methods have become an important route to obtain meaningful structure information on such complexes and make further study of their properties possible.

19-electron complex $[Co(CO)_3(bma)]$ (**3,** Fig. 5(a)) and 19-electron radical anion $[fac\text{-}ReBr(CO)_3(bma)]^-$ (**4**$^-$, Fig. 5(b)) [were both synthesized in laboratories from their 18-electron cationic form, $[Co(CO)_3(bma)]$ (**3**$^+$), and 18-electron neutral form, $[fac\text{-}ReBr(CO)_3(bma)]$ (**4**), respectively [1,2]. According to the IR spectrum, large lower frequency shifts in the carbonyl stretching bands of the bma ligand were observed in both of them, compared with their corresponding 18-electron complexes, respectively [1,2]. The reported experimental bond distances and vibrational frequencies for **3** and **3**$^+$ are listed in Table 3 and Table 9 [1]. The available experimental data on bond angles, bond distances and vibrational frequencies for **4**$^-$ and **4** are also presented in Table 4, Table 6 and Table 10 from the reference paper [2]. Both of the two 19-electron complexes, **3** and **4**$^-$, exhibit the nature of 18+δ

complexes, and the value of δ for the cobalt complex **3** was reported [3]. However, no experimental value of δ was reported for the rhenium complex $\mathbf{2}^-$.

In this work, a B3LYP calculation was carried out on a series of similar complexes to the experimentally known complexes. Cobalt complexes with the chelating ligand 2,3-bisphosphinomaleic anhydride in neutral (**1,** Fig 6(a)) and cationic form ($\mathbf{1}^+$, Fig 6(b)), $[(CO)_3Co(PH_2CC(O)OC(O)CPH_2)]$, representing the 19 and 18 electron systems, respectively, were studied. The same calculation was also performed on rhenium complexes with the same chelating ligand. The anionic form ($\mathbf{2}^-$, Fig 6(c)) and neutral form (**2**, Fig 6(d)), $[(CO)_3ReBr(PH_2CC(O)OC(O)CPH_2)]$, were studied to represent 19 and 18 electron systems, respectively. Due to the complexity of calculation on complexes with phenyl groups, they were ignored in my studied complexes by replacing them with hydrogen atoms. Such replacement is a general practice in computational organometallic chemistry because the phenyl groups are not significant structures in these complexes, and are not expected to have significant effect on calculations.

Computed bond angles, bond distances, natural atomic charges and vibrational frequencies for **1**, $\mathbf{1}^+$, **2** and $\mathbf{2}^-$ are given in Table 3-10, along with their correspondingly available experimentally reported parameters. Differences between the experimental data and computed results are listed, and the differences between the 19-electron systems and the 18-electron systems were also observed and are discussed below. An estimation of the value of δ is given for **1** and $\mathbf{2}^-$, and the value is compared with experimentally determined one.

B. Results and discussions

i. Molecular Geometries

The optimized structures of the cation form **1**$^{+}$ and neutral form **2** are given in Fig. 8 and Fig. 9. Both the cationic **1**$^{+}$/neutral **2**, representing 18-electron complexes, and the neutral **1**/anionic **2**$^{-}$, representing 19-electron complexes are found to be minima.

The data on optimized bond angles for **1**$^{+}$ and **1** are listed in Table 3. It is noted that the bond angles do not change much in these two molecules; the biggest difference is only 2.57 degrees, which means that they both have similar structures. The same trend was also observed for **2** and **2**$^{-}$ (Table 4). The calculated bond angles of **2** and **2**$^{-}$ agree well with the parameters of the correspondingly experimentally known molecules **4** and **4**$^{-}$. The differences between **2** and **4** range from –4.66 to 0.82 degrees, and the differences between **2**$^{-}$ and **4**$^{-}$ range from –8.80 to 5.90. The biggest bond angle difference between studied molecules **2** and **2**$^{-}$ is 4.55 degrees. Thus the ligands in the studied 19-electron system **1** and **2**$^{-}$ do not distort to accommodate the extra electron as a suggested way to stabilize in 19-electron complexes (Chapter I, Section B, [12, 16]).

The calculated and experimentally available bond distances for **1**$^{+}$ and **1** are given in Table 5. Compared the bond distances in **1** with those in the experimentally known analogous **3**, differences between -0.025Å and 0.03Å were observed. The bond involving element P has a difference of 0.03 Å. This is due to the fact that the reference molecule **3** has phenyl groups on P while the computed molecule **1** has hydrogen atoms on P. Bond length differences were observed between computed **1** and **1**$^{+}$. The biggest change

occurs for the C_{10}-C_{11} double bond in the ligand, 2,3-bisphosphinomaleic anhydride; the bond is lengthened by 0.071Å in **1**. The C-C single bonds (C_{11}-C_{13} and C_{10}-C_{12}) around this double bond are shorter in **1** than in $\mathbf{1}^{+}$, the differences are 0.055Å and 0.058Å. The single bonds between P and C (P_8-C_{10} and P_9-C_{11}) around this double bond are also shorter in **1** by 0.058Å and 0.062Å, respectively. It is also noticed that there are some small changes in the C=O double bonds (C_{12}-O_{15} and C_{13}-O_{16}) in the chelating ligand; they are about 0.02 Å longer in **1** than in $\mathbf{1}^{+}$. The C≡O triple bonds of the three carbonyl groups (C_2-O_5, C_3-O_6 and C_4-O_7) are all about 0.006 Å longer in **1**.

Similar bond distance changes were observed in **2** and $\mathbf{2}^{-}$. The calculated data along with the experimental parameters are listed in Table 6. They agree well with each other. The differences between **2** and **4** fall within a range of -0.001Å and 0.048Å, and the differences between $\mathbf{2}^{-}$ and $\mathbf{4}^{-}$ range from –0.013Å to 0.068Å. Therefore, theoretical calculations give good results in bond distances in all studied molecules in this work. For molecules **2** and $\mathbf{2}^{-}$, the most significant change occurs for the C_{11}-C_{12} double bond in the chelating ligand; it is 0.061Å longer in $\mathbf{2}^{-}$ than in **2**. The C-C single bonds around this double bond (C_{11}-C_{17} and C_{12}-C_{18}) are shorter in $\mathbf{2}^{-}$ by 0.042Å. Some big distances change also occur for the P_5-C_{11} and P_6-C_{12} bonds, which are both 0.052Å longer in **2**. In the chelating ligand, some changes were observed for the C_{17}-O_{19} and C_{18}-O_{20} double bonds, which are both 0.024Å longer in $\mathbf{2}^{-}$. The C≡O triple bonds of the three carbonyl groups (C_3-O_9, C_4-O_8 and C_7-O_{10}) are all about 0.006 Å longer in $\mathbf{2}^{-}$. The above bond distance changes in molecules **1** and $\mathbf{2}^{-}$ will be explained in later context.

Table 7 shows natural atomic charges on each element in molecule $\mathbf{1}^+$ and **1**. In general, the atomic charges are lower in **1** than in $\mathbf{1}^+$. The natural charge analysis [4-6] reveals that the most significant charge decreases occur on C_{10}, C_{11}, O_{15} and O_{16} in the ligand; the decreases rang between 0.118 and 0.192 in **1**. The next big decreases occur on O_5, O_6 and O_7 in the three carbonyl groups, which have a decrease between 0.045 and 0.068. The same atomic charge decrease trend was also observed in **2** and $\mathbf{2}^-$. The calculated natural atomic charges for **2** and $\mathbf{2}^-$ are listed in Table 8. Generally, the atomic charges are lower in $\mathbf{2}^-$ than in **2**. The biggest decreases also occur on C_{11}, C_{12}, O_{19} and O_{20} in the ligand, ranging from 0.122 to 0.174. The next big decreases occur on O_8, O_9 and O_{10} in the three carbonyl groups, ranging from 0.043 to 0.051. A more negative the natural atomic charge corresponds to a greater electron population assigned to a given atom. These decreases will be justified later.

ii. Vibrational Frequencies

The scaled IR vibrational frequencies for the carbonyl groups in molecules $\mathbf{1}^+$ and **1** are shown in Table 9, and the scaled frequencies for the carbonyl groups in molecules **2** and $\mathbf{2}^-$ are presented in Table 10. The frequencies for the experimentally known analogues **3**, **4** and $\mathbf{4}^-$ are also shown in these two tables, respectively, as a comparison to the theoretical results. The scale factor 0.9521, which was developed in our group, was used. In both cases, the computed frequencies agree well with available experimental values. The relative error between the theoretical results and

the experimental data is below 1.5% between **1** and **3**, less than 1.0% between **2** and **4**, and less than 1.6% between $\mathbf{2}^-$ and $\mathbf{4}^-$.

The C=O frequencies in the ligand of 2,3-bisphosphinomaleic anhydride in **1** average 90 cm^{-1} lower than those in $\mathbf{1}^+$, and the frequencies of the carbonyl ligands, C≡O, in **1** are about 43 cm^{-1} lower than those in $\mathbf{1}^+$. Such large negative shifts in frequencies are also observed in **2** and $\mathbf{2}^-$. The C=O frequencies in the ligand in $\mathbf{2}^-$ is about 109 cm^{-1} lower than those in **2**, and the frequencies for C≡O have an average of 43 cm^{-1} lower shift in $\mathbf{2}^-$. The higher the frequency, the stronger the bond will be. The large decreases in frequencies of the C=O bonds in the 18-electron complexes, **1** and **2**, indicate that the C=O bonds are weaker than those in the 19-electron complexes, $\mathbf{1}^+$ and $\mathbf{2}^-$.

This phenomenon could be explained as the consequence of a fraction of the electronic charge of the 19^{th} electron moving into the chelating ligand's LUMO (π^*) orbital, which has C=O antibonding character. This weakens the C=O bonds and corresponds to a lower shift in frequencies in the 19-electron complexes, **1** and $\mathbf{2}^-$. Fig. 10 shows the LUMO of $\mathbf{1}^+$. The LUMO is on the chelating ligand. The LUMO lobes have opposite signs, which is an antibonding behavior, between C_{10} and C_{11}, between C_{12} and O_{15}, and between C_{13} and O_{16}. This antibonding character results in the longer bond distances in the bonds of C_{11}-$C_{12,}$ C_{12}-O_{15} and C_{13}-O_{16} in the neutral form **1** (as mentioned earlier in the chapter). The molecular orbitals have the same sign between C_{11}-C_{13} and C_{10}-$C_{12,}$ so they form bonding orbitals, which result in shorter bond distances in molecule **1**. Same frequency analyses could be applied to the rhenium complex. The delocalization of the 19^{th} valence

electron onto the chelating ligand's LUMO, which has antibonding behavior, results in lengthening the bond distances between C_{11}-C_{12}, C_{17}-O_{19} and C_{18}-O_{20} in **2**$^-$. And the bonding behavior in the bonds of C_{11}-C_{17} and C_{12}-C_{18} shortens their bond distances in **2**$^-$. Therefore, it can be established that the unpaired, 19th electron is distributed partly onto the 2,3-bisphosphinomaleic anhydride ligand in **1** and **2**$^-$. As Table 9 and 10 show, there are also some lower frequency shifts in the carbonyl ligands C≡O in **1** and **2**$^-$. This indicates that a portion of the 19th electron is also delocalized onto the metal fragments in each complex. Therefore, the 19-electron complex, **1** and **2**$^-$, can actually be classified as an 18+δ system, where $0<\delta<1$ with the 19th electron is distributed on both the chelating ligand and the metal. Comparing the magnitude of the frequency decreases of C=O and carbonyl groups C≡O, there should be a greater electron fraction on the ligand than on the metal. The more significant atomic charge decreases on C_{10}, C_{11}, O_{15} and O_{16} in the chelating ligand in **1** (C_{11}, C_{12}, O_{19} and O_{20} in **2**$^-$), and relative smaller charge decreases on O_5, O_6 and O_7 in **1** (O_8, O_9 and O_{10} in **2**$^-$), are consistent with this conclusion.

iii. Measurement of δ

So far, the results and discussion above show that the molecules **1** and **2**$^-$ have the nature of 18+δ complexes. The next job is to obtain a quantitative value of δ to show what fraction of the 19th electron has been moved onto the ligand and how much still stays on the metals. An infrared spectroscopic method for measuring δ in 18+δ organometallic complexes, containing 2,3-

bis(diphenylphosphino)maleic anhydride (L_2') and 2,3-bis(diphenylphosphino)-2-cyclopentene-1,4-dione (L_2'') (Chapter I, Fig 4) was devised by Schut, D.M. *et al* [3]. In comparing the 18- with 19-electron complexes, if the additional charge of the 19-electron complex is completely centered on L_2', the C=O vibrational frequencies should be those of the anionic ligand L_2'$^-$. Conversely, if none of the extra charge is found on L_2', the C=O vibrational frequencies should be equal to those of L_2'. In practice, the C=O vibrational frequencies of 18+δ complexes containing L_2'-type ligands occur between the L_2' and L_2'$^-$ limits, reflecting a charge on L_2' between 0 and –1. A linear relationship between C=O force constants and the charge on a ligand is given by [Eq. 3.1] [7-9]

$$k = k_0 + k'q \qquad \text{[Eq. 3.1]}$$

where k_0 is the force constant when the charge q=0, and k_0 + k' is the force constant when q=-1. The frequency is proportional to the square root of the force constant; thus

$$\bar{\upsilon} = \sqrt{a + bq} \qquad \text{[Eq. 3.2]}$$

where a and b are constants related to k_0 and k'. Squaring each side of Eq. 3.2 and subtracting the results for two different molecules yields

$$\bar{\upsilon}_2^{\,2} - \bar{\upsilon}_1^{\,2} = b\Delta q \qquad \text{[Eq. 3.3]}$$

where $\bar{\upsilon}_2$ and $\bar{\upsilon}_1$ are the C=O vibrational frequencies of the 18+δ and 18-electron complexes, and Δq is the difference in charge on the L_2 ligand between the 18-electron and the 18+δ complexes. The value of δ is equal to 1+Δq. If Δq=-1, the electron is completely centered on the ligand, therefore δ=0. Likewise, if Δq=0, the electron is completely metal centered, δ=1.

The above method is applied to the measurement of δ in this work. The molecular structure of studied chelating ligand, L_2, is shown in Fig 7. The constant b was determined by substituting the C=O frequencies for the L_2 and L_2^- species into Eq. 3.3 and setting Δq=-1. The b values for experimental L_2'/L_2'$^-$ and theoretical L_2/L_2^- are given in Table 11. With b determined, values for Δq and δ were determined by substituting the appropriate frequencies of the 18-electron and 18+δ systems (listed in Table 12) into Eq. 3.3. According to the reference [3], root mean square (rms) frequencies were used to calculate the value for δ because the two different frequencies for C=O in each molecule didn't give consistent δ values. The resulting values of Δq and δ for **1** and **2**$^-$ are given in Table 13. The experimentally known δ value for **3** is also given in the same table. The calculated δ value (δ=0.21) for **1** agrees very well with that of experimentally known **3** (δ =0.19). δ is calculated to be 0.10 for **2**$^-$. Because δ<<1, the 19th electron largely localized onto metals in the studied 18+δ systems **1** and **2**$^-$.

The above mentioned method needs reference molecules (means free ligand) to calculate the value of δ. However, we have used another more general method to calculate δ using atomic charges. By nature, all the electrons in a molecule will be distributed over the entire molecule according to the electronegativities of the individual atoms. This leads to atomic charges on individual atoms in the molecule. Let us say q_{18} is the sum of all the atomic charges on the chelating ligand part of the 18-electron complex. Similarly, q_{19} will be the sum of all the atomic charges on chelating ligand part of the 19-electron complex. The difference between q_{19} and q_{18} should be the

Δq, the charge difference on the chelating ligand between 18-and 19-electron complexes; then the value of δ equals to 1+Δq. On the other hand, the value of δ can also be calculated in a similar way by taking the metal and all other non-chelating ligands into the account; the charge difference on the sum of those atoms between 18- and 19-electron complexes is the value of δ. Though the experimental measurement of atomic charges in a molecule is very difficult and can only be possible by X-ray diffraction methods, the theoretical calculation of atomic charges is done quite regularly. In the present work, we have used natural atomic charges to calculate δ and Δq, and compare the values with those obtained by the frequency method. The results are given in parentheses in Table 13.

The calculated values of δ for **1** and **2**$^-$ by two different theoretical methods agree reasonably well with each other. The calculated value of δ for **1** also agrees quite well with the experimentally known molecule **3**. Although currently there has been no experimental parameter available for rhenium complex **2**$^-$, we believe that the calculated δ makes a good prediction with regard to the results for the cobalt complex **1**.

C. Conclusions

The cobalt complexes, $[(CO)_3Co(PH_2CC(O)OC(O)CPH_2)]$, in cationic (**1**$^+$) and neutral (**1**) forms were studied as 18- and 19-electron systems. The rhenium complexes, $[(CO)_3ReBr(PH_2CC(O)OC(O)CPH_2)]$, in neutral (**2**) and anionic (**2**$^-$) forms were also studied as 18- and 19-electron systems. The 19-electron complexes, **1** and **2**$^-$, can actually be classified as 18+δ systems.

Both the 18-electron and 18+δ systems have similar structures. The theoretical results agree well with the experimentally available data on bond angles, bond distances and vibrational frequencies. With the calculated values of δ for molecules **1** and $\mathbf{2}^-$, conclusion could be made that the 19th electron is mostly distributed over the chelating ligand of 2,3-bisphosphinomaleic anhydride and partially localized onto the metals in **1** and $\mathbf{2}^-$.

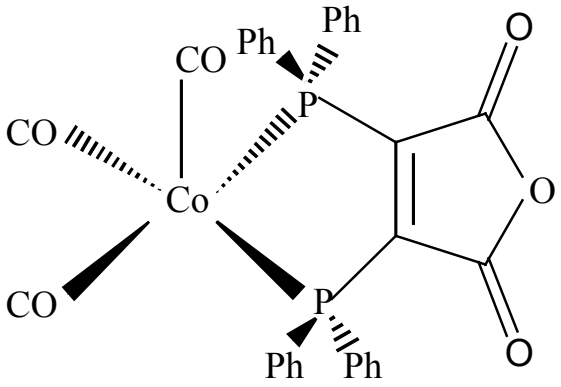

(a)

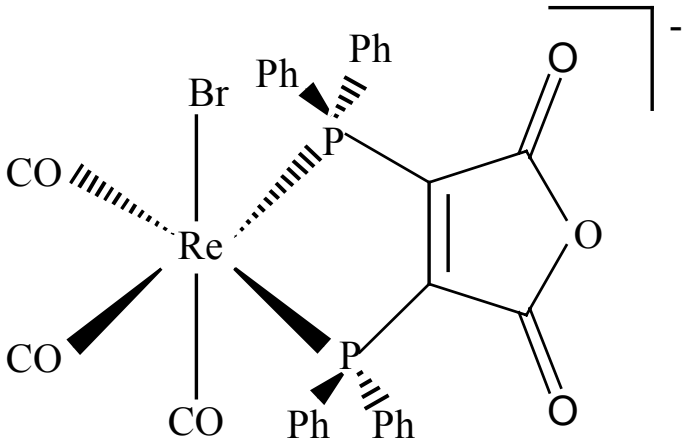

(b)

Figure 5 Molecular structures of experimentally known complexes
(a) 19-electron complex **3** $[(CO)_3Co(PH_2CC(O)OC(O)CPH_2]$
(b) 19-electron complex **4**$^-$ $[(CO)_3ReBr(PH_2CC(O)OC(O)CPH_2]^-$

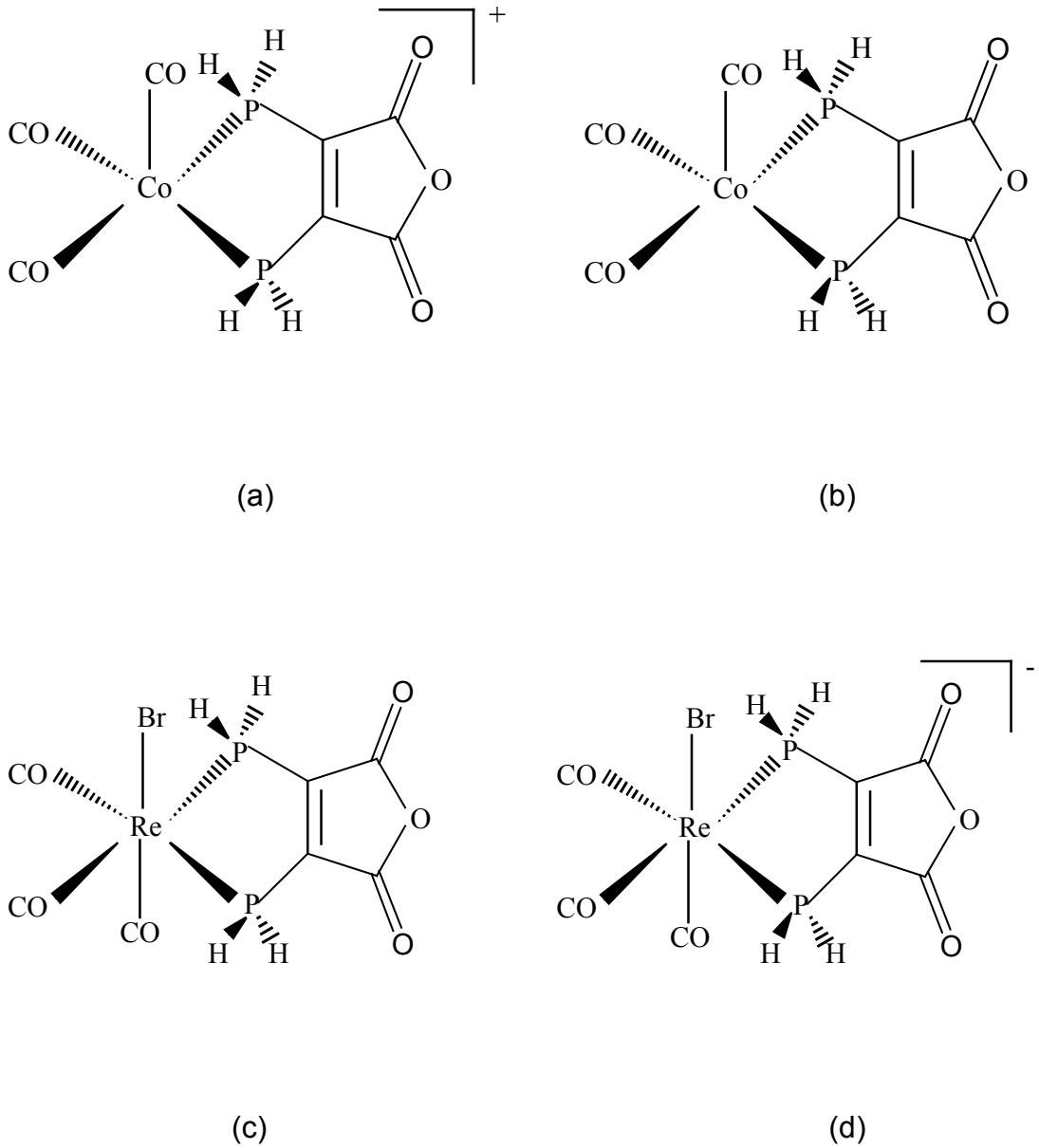

Figure 6 Molecular structures of studied complexes
(a) 18-electron complex **1**$^{+}$ $[(CO)_3Co(PH_2CC(O)OC(O)CPH_2)]^{+}$
(b) 19-electron complex **1** $[(CO)_3Co(PH_2CC(O)OC(O)CPH_2)]$
(c) 18-electron complex **2** $[(CO)_3ReBr(PH_2CC(O)OC(O)CPH_2)]$
(d) 19-electron complex **2**$^{-}$ $[(CO)_3ReBr(PH_2CC(O)OC(O)CPH_2)]^{-}$

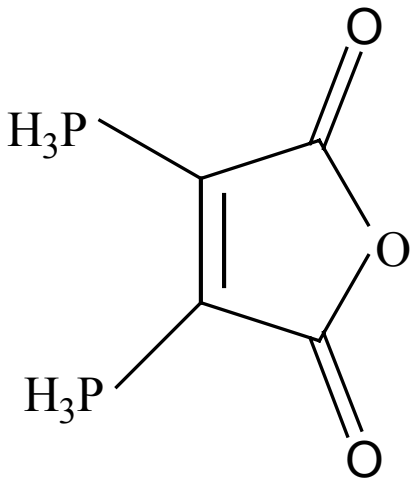

Figure 7 Molecular structure of ligand L_2

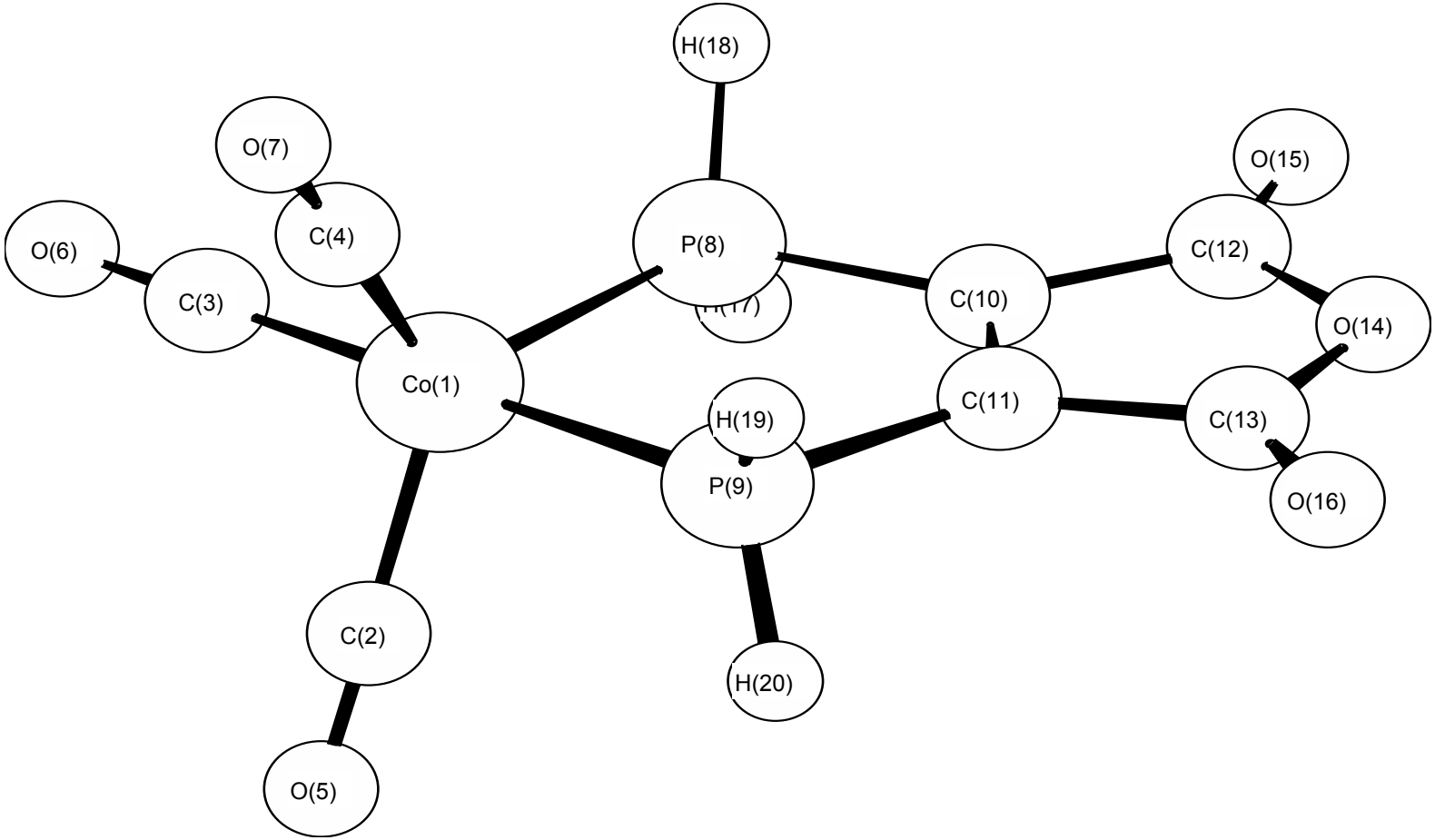

Figure 8 The optimized structure of $\mathbf{1}^{+}$ at B3LYP level

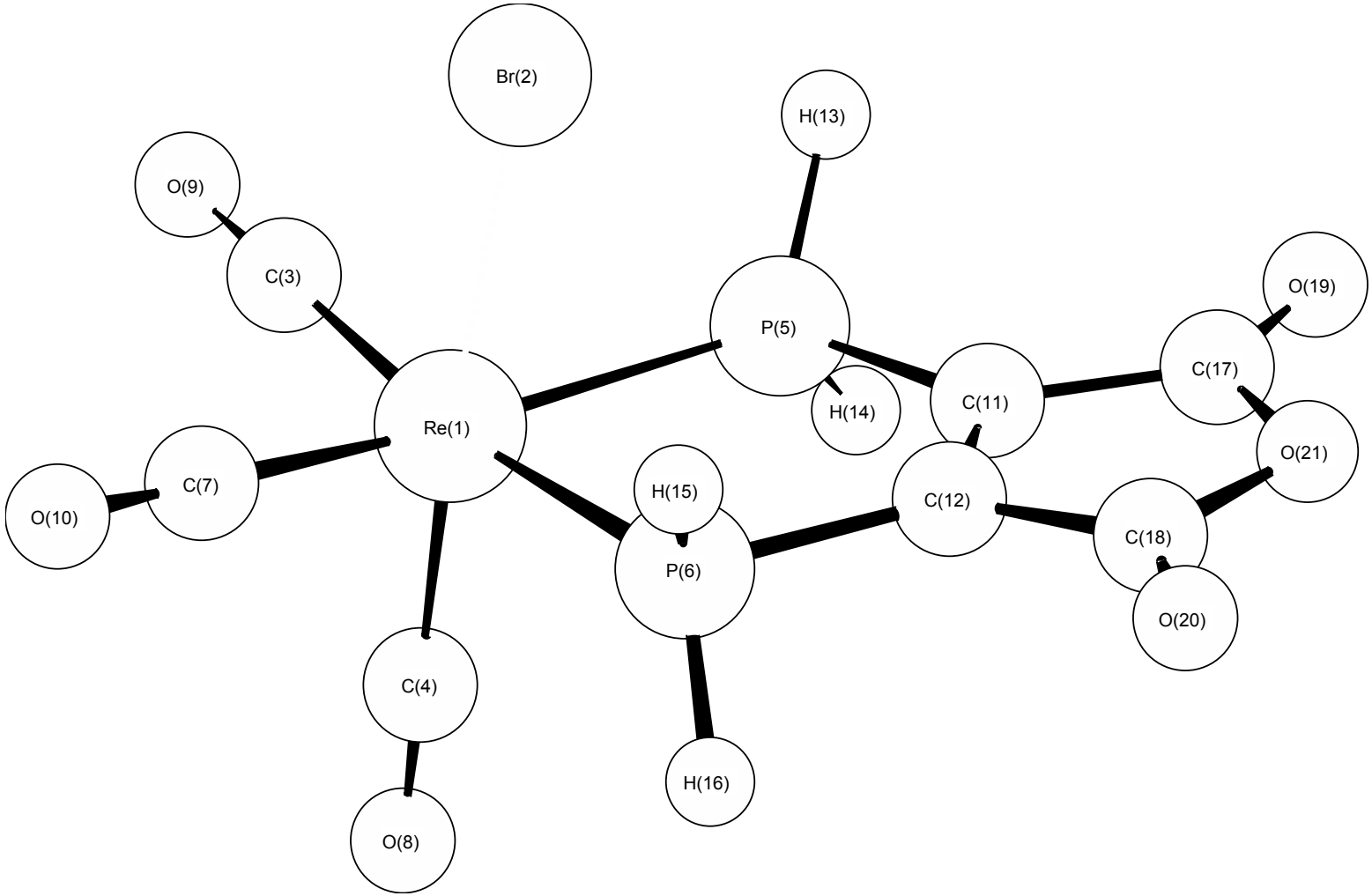

Figure 9 The optimized structure of **2** at B3LYP level

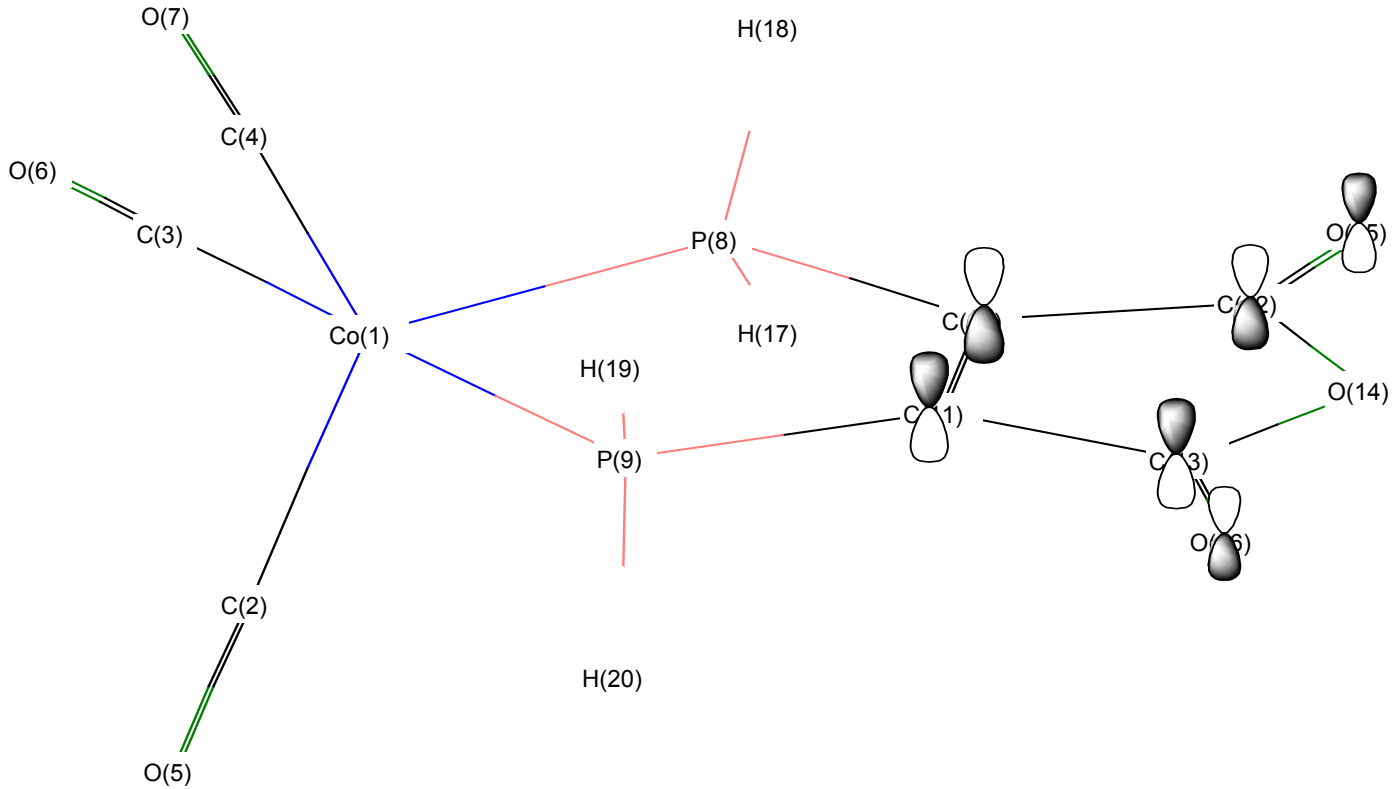

Figure 10 Lowest unoccupied molecular orbital (LUMO) for **1**$^{+}$

Table 3. Optimized Bond Angles of Molecules **1**$^{+}$ and **1**

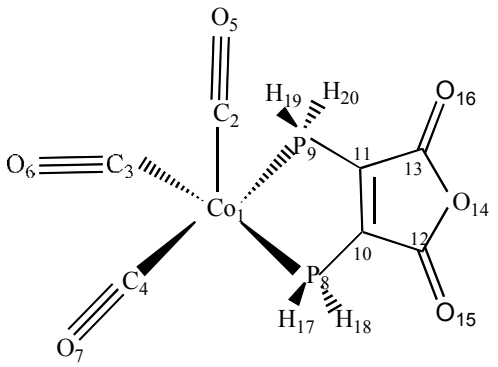

	Bond Angles (degree)	
	1^{+}	**1**
C2-Co-C3	90.86	93.43
C2-Co-C4	127.45	126.07
C2-Co-P8	116.22	116.82
C2-Co-P9	89.60	88.67
P8-Co-P9	87.51	86.61
Co-P8-C10	105.20	106.45
Co-P9-C11	106.48	107.95
C10-C12-O14	106.89	106.59
C11-C13-O14	106.65	106.45
C10-C12-O15	128.84	130.87
C11-C13-O16	128.77	131.21
C13-O14-C12	110.02	110.64
C10-C11-C13	108.50	108.47
C11-C10-C12	107.73	107.35
H17-P8-H18	98.64	97.58
H19-P9-H20	100.42	98.35

Table 4. Optimized Bond Angles of Molecules **2** and **2**$^{-}$, and Experimental Bond Angles of Molecules **4** and **4**$^{-}$

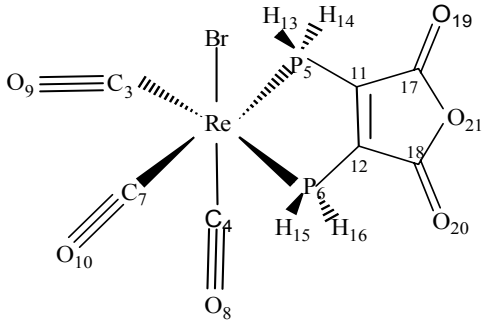

	Bond Angles (degree)						
	4	**2**	Δ (2-4)	**4**$^{-}$	**2**$^{-}$	Δ (2^{-}- 4^{-})	Δ (2-2^{-})
Br-Re-C3	90.05	90.87	0.82	85.64	89.63	3.99	1.24
Br-Re-C4	178.55	175.84	-2.71	173.83	177.27	3.44	-1.44
Br-Re-P5	86.21	81.55	-4.66	85.90	85.07	-0.83	-3.51
Br-Re-P6	82.01	81.56	-0.45	92.70	86.10	-6.60	-4.55
Br-Re-C7	89.55	90.87	1.32	98.44	89.64	-8.80	1.23
P5-Re-P6	83.12	82.94	-0.18	84.21	81.14	-3.07	1.80
Re-P5-C11	103.95	106.02	2.07	105.64	107.69	2.05	-1.67
Re-P6-C12	103.76	106.03	2.27	106.05	107.69	1.64	-1.66
P5-Re-C3	96.75	92.39	-4.36	94.34	92.80	-1.54	-0.41
P6-Re-C7	90.08	92.39	2.31	92.55	92.80	0.25	-0.41
P5-Re-C4	92.35	95.34	2.99	87.93	93.04	5.11	2.30
P6-Re-C4	98.26	95.34	-2.92	87.13	93.03	5.90	2.31
P5-C11-C12	122.10	121.83	-0.27	121.89	121.29	-0.60	0.54
P6-C12-C11	121.10	120.74	-0.36	121.10	120.72	-0.38	0.01
C12-C11-C17	108.20	107.99	-0.21	108.10	108.12	0.02	-0.14
C11-C12-C18	108.10	107.90	-0.20	107.10	108.11	1.01	-0.20
C11-C17-O21	107.10	107.38	0.28	107.10	106.94	-0.16	0.44
C17-O21-C18	109.10	109.06	-0.04	109.10	109.87	0.77	-0.81
O21-C18-C12	109.10	107.39	-1.71	108.10	106.94	-1.16	0.45

Table 5. Optimized Bond Distance of Molecules **1**$^{+}$ and **1**, and Experimental Bond Distances of Moleucle **3**

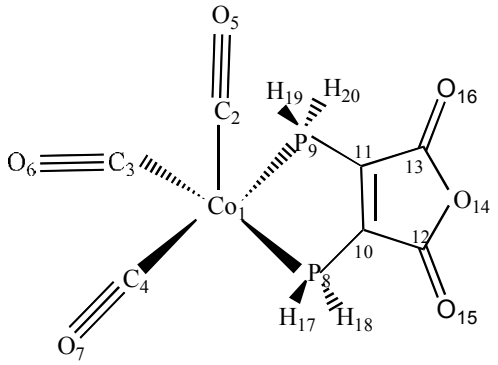

Bond Type	Bond Distance (Å)				
	1^{+}	**1**	**3**	Δ (1-3)	Δ (1^{+}-1)
Co-C2	1.831	1.809	1.833	-0.024	0.023
Co-C3	1.815	1.791	1.783	0.008	0.023
Co-C4	1.831	1.809			0.023
Co-P8	2.318	2.315			0.003
Co-P9	2.280	2.290	2.260	0.030	-0.010
C2-O5	1.142	1.149	1.134	0.015	-0.006
C3-O6	1.139	1.146	1.141	0.005	-0.007
C4-O7	1.142	1.149			-0.006
P8-C10	1.823	1.765			0.058
P9-C11	1.816	1.754	1.779	-0.025	0.062
C10-C11	1.339	1.410	1.386	0.024	-0.071
C10-C12	1.505	1.447			0.058
C11-C13	1.503	1.448	1.435	0.013	0.055
C12-O14	1.391	1.409			-0.018
C13-O14	1.388	1.403	1.417	-0.014	-0.015
C12-O15	1.192	1.213			-0.020
C13-O16	1.193	1.213	1.209	0.004	-0.020

Table 6. Optimized Bond Distances of Molecules **2** and **2**$^{-}$, and Experimental Bond Distances of Molecules **4** and **4**$^{-}$

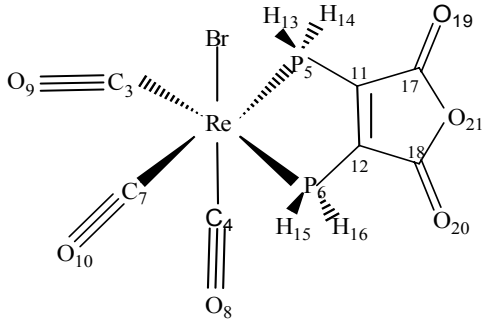

Bond Type	Bond Distance (Å)						
	4	**2**	Δ (2-4)	**4**$^{-}$	2^{-}	Δ (2^{-}-4^{-})	Δ (2-2^{-})
Re-Br	2.638	2.673	0.035	2.626	2.685	0.059	-0.012
Re-C3	1.952	1.965	0.013	1.942	1.952	0.01	0.013
Re-C4	1.881	1.929	0.048	1.900	1.917	0.017	0.012
Re-P5	2.441	2.471	0.030	2.467	2.487	0.02	-0.016
Re-P6	2.458	2.471	0.014	2.463	2.487	0.024	-0.016
Re-C7	1.932	1.965	0.033	1.901	1.952	0.051	0.013
C3-O9	1.153	1.153	0.000	1.162	1.161	-0.001	-0.007
C4-O8	1.162	1.162	0.000	1.101	1.169	0.068	-0.006
C7-O10	1.152	1.153	0.001	1.182	1.161	-0.021	-0.007
P5-C11	1.832	1.831	-0.001	1.792	1.780	-0.013	0.052
P6-C12	1.822	1.831	0.009	1.781	1.780	-0.001	0.052
C11-C12	1.342	1.341	-0.001	1.412	1.402	-0.01	-0.061
C11-C17	1.503	1.496	-0.007	1.432	1.454	0.022	0.042
C12-C18	1.483	1.496	0.013	1.422	1.454	0.032	0.042
C17-O21	1.402	1.393	-0.009	1.402	1.409	0.007	-0.016
C18-O21	1.382	1.393	0.011	1.412	1.409	-0.003	-0.016
C17-O19	1.192	1.197	0.005	1.202	1.221	0.019	-0.024
C18-O20	1.182	1.197	0.015	1.212	1.221	0.009	-0.024

Table 7. Natural Atomic Charges of Molecules **1**$^{+}$ and **1**

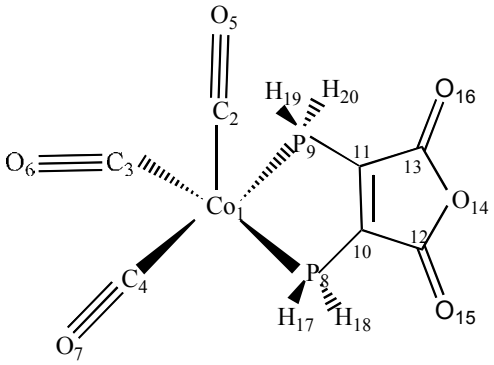

Element Number	Atomic charge		Difference
	1^{+}	**1**	Δ (1^{+}-1)
Co	-0.141	-0.159	0.018
C2	0.469	0.450	0.019
C3	0.568	0.539	0.029
C4	0.469	0.450	0.019
O5	-0.377	-0.422	0.045
O6	-0.345	-0.412	0.068
O7	-0.376	-0.422	0.046
P8	0.423	0.486	-0.064
P9	0.569	0.645	-0.075
C10	-0.360	-0.539	0.179
C11	-0.394	-0.585	0.192
C12	0.812	0.771	0.041
C13	0.811	0.780	0.031
O14	-0.518	-0.550	0.032
O15	-0.451	-0.569	0.118
O16	-0.460	-0.578	0.118
H17	0.073	0.029	0.044
H18	0.073	0.030	0.043
H19	0.076	0.029	0.048
H20	0.076	0.028	0.049

Table 8. Natural Atomic Charges of Molecules **2** and **2**$^{-}$

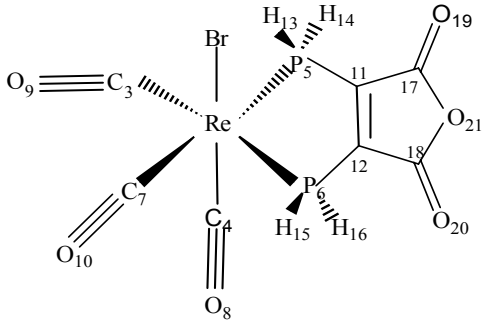

Element Number	Atomic charge		Difference
	2	**2**$^{-}$	Δ (2-2^{-})
Re	-0.619	-0.532	-0.087
Br	-0.486	-0.530	0.044
C3	0.604	0.578	0.026
C4	0.530	0.527	0.003
P5	0.550	0.565	-0.015
P6	0.550	0.566	-0.016
C7	0.604	0.577	0.027
O8	-0.459	-0.502	0.043
O9	-0.426	-0.476	0.051
O10	-0.426	-0.477	0.051
C11	-0.366	-0.540	0.174
C12	-0.366	-0.537	0.171
H13	0.061	0.020	0.041
H14	0.038	0.005	0.033
H15	0.061	0.023	0.038
H16	0.038	0.006	0.032
C17	0.818	0.764	0.054
C18	0.818	0.762	0.056
O19	-0.493	-0.615	0.122
O20	-0.493	-0.615	0.122
O21	-0.539	-0.567	0.029

Table 9. Scaled Vibrational Frequencies of C≡O and C=O for Molecules **1**$^{+}$ and **1,** and Experimental Vibrational Frequencies of Molecules **3**

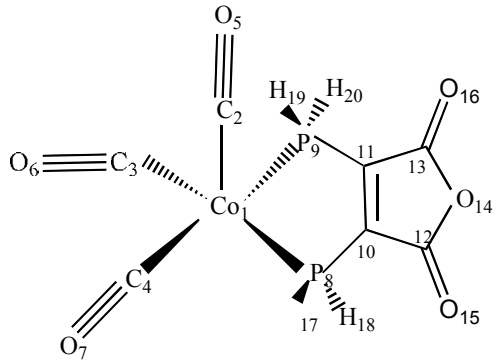

Group	Frequency (cm^{-1})				
	1^{+}	**1**	**3**	Δ (1-3)	Δ (1^{+}-1)
C=O	1784.6	1695.7	1670.0	25.7	88.9
	1838.9	1746.6	1740.0	6.6	92.3
C≡O	2047.9	2004.3	2015.0	-10.7	43.6
	2065.6	2019.5			46.1
	2096.4	2056.6	2075.0	-18.4	39.8

Table 10. Scaled Vibrational Frequencies of C≡O and C=O for Molecules **2** and **2**$^{-}$, and Experimental Vibrational Frequencies for Molecules **4** and **4**$^{-}$

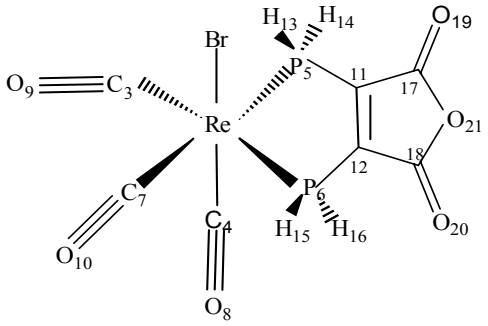

Group	Frequency (cm^{-1})						
	2	**4**	Δ (2- 4)	**2**$^{-}$	**4**$^{-}$	Δ (2^{-}- 4^{-})	Δ (2-2^{-})
C=O	1774.4	1778	-3.6	1670	1649	21	109.7
	1829.4	1848	-18.6	1725.6	1730	-4.4	109
CºO	1932.9	1920	12.9	1894.4	1905	-10.6	40.4
	1975.5	1975	0.5	1926.9	1943	-16.1	51.1
	2028.4	2045	-16.6	1992.9	2026	-33.1	37.3

Table 11. b values for experimental ligand L_2' and for L_2 by using C=O vibrational frequencies obtained from Table 12 and Eq. 3.3

	couple	b (cm^2)
Experimental [a]	$L_2'/L_2'^-$	4.32E+05
Theoretical	L_2/L_2^-	4.07E+05

[a] Reference [3]. The molecular structure for L_2' is shown in Chapter 1, Fig 4.

Table 12. Experimental and calculated C=O vibrational frequencies used for calculating δ

	complex	Freq(C=O),cm^{-1}	Freq$(C=O)_{rms}$,cm^{-1}
Experimental [a]	L_2'	1835 1765	1800
	L_2'$^-$	1716 1635	1676
	3	1746 1679	1713
	3$^+$	1846 1778	1812
Theoretical	L_2	1751.5 1698.5	1725.2
	L_2^-	1652.1 1552.1	1602.9
	1	1746.6 1695.7	1721.3
	1$^+$	1838.9 1784.6	1812.0
	2	1829.4 1774.4	1802.1
	2$^-$	1725.6 1670.0	1698.0

[a] Reference [3]. The molecular structure for L_2' is shown in Fig 4. The molecular structure for **3** is shown in Fig 5(a).

Table 13. Experimental and calculated values of Δq and δ, using C=O vibrational frequencies from Table 12 and b values from Table 11

	Couple	Δq[b]	δ
Experimental [a]	**3**/**3**$^{+}$	-0.81	0.19
Theoretical	**1**/**1**$^{+}$	-0.79 (-0.76)	0.21(0.24)
	2^{-}/**2**	-0.9 (-0.84)	0.10(0.16)

[a] Reference [3]. The molecular structure for L_2' is shown in Fig 4. The molecular structure for **3** is shown in Fig 5(a).

[b] The numbers in the parentheses are the results from natural atomic charges, NBO analysis

CHAPTER REFERENCE

1. Fenske D., *Angew. Chem. Int. Ed. Engl*. 1976, *15*, No. 6, 381
2. Yang K.Y., Bott S.G. and Richmond M.G., *Organometallics.* 1995, *14*, 2387
3. Schut D.M., Keana K.J., Tyler D.R. and Rieger P.H., *J. Am. Chem. Soc.* 1995, *117*, 8939
4. Foster J. P., Weinhold, F., J. Am. Chem. Soc. 1980, 102, 7211-7218
5. Reed A.E., Curtiss, L.A. and Weinhold F., Chem. Rev. 1988, 899-926
6. Reed A.E., Weinhold, F., F. QCPE Bull., 1985, 5, 141
7. (a) Timmy J.A., *Inorg. Chem*. 1979, *18*, 2502. (b) Mines. G.A., Roberts. J.A. and Hupp. J.T., *Inorg. Chem*. 1992, *31*, 125
8. (a) Haas. H., Sheline. R.K., *J. Chem. Phys*. 1967, 47, 2996. (b) Graham. W.A.G., *Inorg. Chem*. 1968, *7*, 315
9. Chappell. J.S., Bloch. A.N., Bryden. W.A., Maxfield. M., Poehler. T.O. and Cowan. D.O., *J. Am. Chem. Soc*. 1981, *103*, 2442

BIBLIOGRAPHY

Andzelm J., Wimmer E., *J. Chem. Phys.* 1992, *96*, 1280

Astruc D., *Chem. Rev*. 1988, *88*, 1189

Becke A.D., *J. Chem. Phys.* 1992, *96*, 2155; 1992, *97*, 9173

Becke A.D., *J. Chem. Phys*. 1993,*98* 5648

Becke A.D., *Phys. Rev. A* 1986, *33*, 2786

Becke A.D., *Phys. Rev.,* 1988, *38*, 3098

Boys S.F., *Proc. Roy. Soc. (London)*, 1950, *A200*, 542

Braden D.A., Tyler D.R., *J. Am. Chem. Soc*. 1998, *120*, 942

Braden D.A., Tyler D.R., *Organometallics*, 2000, *19*, 3762

Brown T.L., *In Organometallic Radical Processes*; Trogler W.C., Ed.; Elsevier: New York, 1990, *67*

Castellani M.P., Tyler D.R., *Organometallics* 1989, *8*, 2113

Chappell. J.S., Bloch. A.N., Bryden. W.A., Maxfield. M., Poehler. T.O. and

Cowan. D.O., *J. Am. Chem. Soc*. 1981, *103*, 2442

Colle R., Salvetti O., *J. Chem. Phys.* 1983, *79*, 1404 and references therein

Collman J.P., Hegedus L.S., Norton J.R. and Finke R.G., *Principles and Applications of Organotransition Metal Chemistry,* 1987

Cundari T.R., Benson M.T., Lutz M.L. and Sommerer S.O., *Rev. Comput. Chem*. 1996, *8*, 145

Curtiss L.A., Raghavachari K., Trucks G.W. and Pople J.A., *J. Chem. Phys*. 1990, *93*, 2537

Duffy N.I.W., Nelson R.R., Richmond M.G., Rieger A.L., *Inorg. Chem*. 1998, *37*, 4849

Dyall K., *J. Chem. Phys*. 1991, *96*, 1210

Fenske D., *Angew. Chem. Int. Ed. Engl*. 1976, *15*, No. 6, 381

Foresman J.B., *Exploring chemistry with electronic structure methods*, 2nd edition, Gaussian, Inc, 1996

Foster J. P., Weinhold, F., J. Am. Chem. Soc. 1980, 102, 7211-7218

Foster, J. P., Weinhold, F., J. Am. Chem. Soc., 1980, 102, 7211-7218

Frenking G., Antes I., Böhme M., Dapprioh S., Ehlers A.W., Jonas V., Nauhaus A., Otto M., Stegmann R., Veldkamp A. and Vyboishchikov S.F., *Rev. Comput. Chem.* 1996*, 8*, 63

Gaussian 98, Revision A.9, Frisch, M.J., Trucks, G.W., Schlegel, H. B., Scuseria, G.E., Robb, M.A., Cheeseman, J.R., Zakrzewski, V.G., Montgomery, J.A., Stratmann, Jr.,R.E., Burant, J.C., Dapprich S., Millam, J.M., Daniels, A.D., Kudin, K.N., Strain, M.C., Farkas, O., Tomasi, J., Barone, V., Cossi, M., Cammi, R., Bennucci, B., Pomelli, C., Adamo, C., Clifford, S., Ochterski, J., Petersson, G.A., Ayala, P. Y., Cui, Q., Morokuma, K., Malick, D.K., Rubuck, A.D., Raghavachari, K., Foresman, J.B., Cioslowski, J.J., Ortiz, V.A., Baboul, G., Stefanov, B. B., Liu, G., Liashenko, A., Piskorz, P., Komaromi, I., Gomperts, R., Martin, R.L., Fox, D.J., Keith, T., Al-Laham, M.A., Peng, C.Y., Nanayakkara, A., Challacombe,M., P. Gill, M.W., Johnson, B., Chen, W., Wong, M.W., Andres, J.L., Gonzalez, C., Head-Gordon, M., Replogle, E. S. and Pople, J. A. Gaussian, Inc., Pittsburgh PA, 1998.

Geiger W.E., *Acc. Chem. Res*. 1995, *28*, 351

Geiger W.E., Gennett T., Lane G.A., Slazer A. and Rheingold A.L., *Organometallics* 1986, *5*, 1352

Graham. W.A.G., *Inorg. Chem*. 1968, *7*, 315

Gunnarsson O., Lundquist I., *Phys. Rev*. 1976, *B13,* 4274

Haas. H., Sheline. R.K., *J. Chem. Phys*. 1967, 47, 2996

Hay P.J., Wadt W.R., *J. Chem. Phys*. 1982, *77*, 3654

Herrinton T.R., Brown T.L., *J. Am. Chem. Soc.* 1985, *107*, 5700

Hohenberg P., Kohn W., *Phys. Rev*. 1964, *136*, B864

Jensen F., *Introduction to Computational Chemistry*, Wiley, 1999

Johnson B.G., Gill P.M.W. and Pople J.A., *J. Chem. Phys*. 1993, *98*, 5612

Kristyan S., Pulay P., *Chem. Phys. Lett.* 1994, *229*, 175

Lee C., Yang W. and Parr R.G., *Phys. Rev. B.* 1988, *37*, 785

Lionel T., Morton J.R., Preston K.F., *Chem. Phys. Lett*. 1981, *81*, 17

Lipkowitz K.B., Boyd D.B., *Reviews in computational chemistry*, 1996, *8*, 63

Mao F., Tyler D.R., Bruce M.R.M., Bruce A.E., Rieger A.L. and Rieger P.H., *J. Am. Chem. Soc.* 1992, *114*, 6418

Mao F., Tyler D.R., Rieger A.L., Rieger P.H., *J. Chem. Soc*., Faraday Trans., accepted for publication.

Miessler G.L., *Inorganic Chemistry*, 2nd Edition, 1998

Mines. G.A., Roberts. J.A. and Hupp. J.T., *Inorg. Chem*. 1992, *31*, 125

Narayanan B.A., Kochi J.K., *J. Organomet. Chem*. 1984, *272*, C49

Olbrich-Deussner B., Kaim W., *J. Organomet. Chem.* 1988, *340,* 71

Parr R.G., Yang W., *Density Functional Theory*, Oxford University Press, 1989

Peake B.M., Symons M.C.R. and Wyatt J.L., *J. Chem. Soc*., *Dalton Trans*. 1983, 1171

Perez-Jorda J.M., Becke A.D., *Chem. Phys. Lett*. 1995, *233*, 134

Philbin C.E., Granatir C.A. and Tyler D.R., *Inorg. Chem*. 1986, *25*, 4806

Pople J.A., Head-Gordon M, Fox D.J., Raghavachari K. and Curtiss L.A, *J. Chem. Phys*. 1989, *90*, 5622

Reed A.E., Curtiss, L.A. and Weinhold F., Chem. Rev. 1988, 899-926

Reed A.E., Weinhold, F., F. QCPE Bull., 1985, 5, 141

Reed, A.E., Curtiss, L.A. and Weinhold F., Chem. Rev., 1988, 899-926

Reed, A.E., Weinhold, F., F. QCPE Bull., 1985, 5, 141

Schut D.M., Keana K.J., Tyler D.R. and Rieger P.H., *J. Am. Chem. Soc.* 1995, *117*, 8939

Schut D.M., Tyler D.R., Rieger P.H., *J. Am. Chem. Soc.* 1995, *117*, 8939

Sim F., St-Amant A., Papai I. And Salahub D.R., *J. Am. Chem. Soc*. 1992, *114*, 4391

Slater J.C., *Phys. Rev*. 1930, *36,* 57

Stevens W., Krauss J.M., Basch H. and Jasien P.G., *Can. J. Chem*. 1992, *70,* 612

Therien M., Trogler W.C., *J. Am. Chem. Soc.* 1987, *109*, 5127

Timmy J.A., *Inorg. Chem*. 1979, *18*, 2502.

Tyler D.R., *Acc. Chem. Res*. 1991, *24*, 325

Tyler D.R., In *Organometallic Radical Processes*; Trogler W.C., Ed.; Elsevier: New York, 1990, 338

Tyler D.R., Mao F., *Coord. Chem. Rev*. 1990, *97*, 119

Tyler D.R., *Prog. Inorg. Chem*. 1988, *36*, 125

von Barth U., Hedin L., *Phys. Rev.* 1979, *A20*, 1693

Vosko S.J., Wilk L. and Nusair M., Can. *J. Phys.* 1980,*58*, 1200

Weil J.A., Bolton J.R., Wertz J.E., *Electron Paramagnetic Resonance*; Wiley: New York, 1994

Yang K.Y., Bott S.G. and Richmond M.G., *Organometallics.* 1995, *14*, 2387

Zhang Y., Gosser D.K., Rieger P.H. and Sweigart D.A., *J. Am. Chem. Soc*. 1991, *113*, 4062